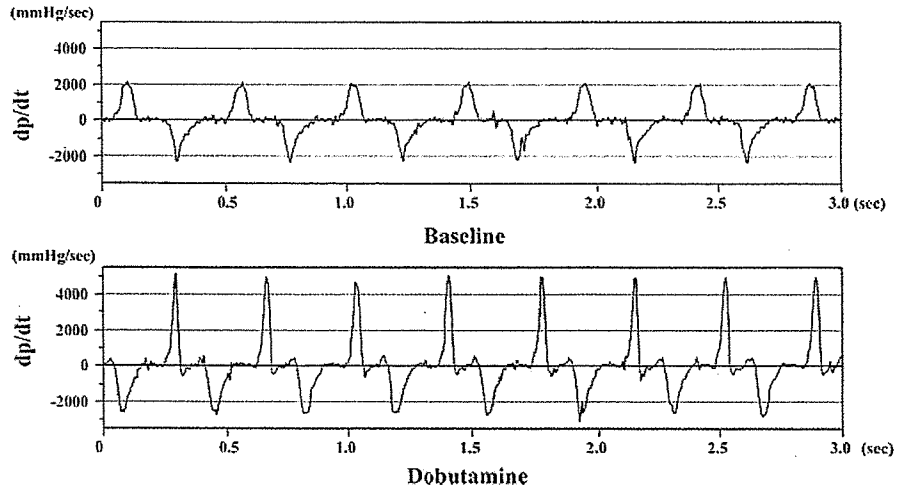

Fig. 4. dP/d*t* waveform before (*top*) and after (*bottom*) dobutamine infusion.

Reproducibility. Myocardial strain was measured by two independent observers and by one observer two times a week apart in 10 randomly selected segments to determine interobserver and intraobserver variability. The variability was assessed as the absolute difference between two measurements expressed as a percentage of their mean values. The interobserver variability was 6.5 ± 5.5 and 9.5 ± 7.5% for the subendocardial and subepicardial strains, respectively. The intraobserver variability was 7.2 ± 4.9 and 9.3 ± 3.7% for the subendocardial and subepicardial strains, respectively.

Statistical analysis. Hemodynamic data were obtained as an average of three to five consecutive beats. Statistical analyses were done with commercially available software (StatView 5.0; SAS Institute). Data are expressed as mean values ± SD. Comparisons of parameters among the stages were made by one-way ANOVA for repeated measures, followed by Scheffé's test. The Wilcoxon signed-ranks test was used to compare parameters before and after DSE. $P < 0.05$ was considered to indicate statistical significance.

RESULTS

Hemodynamic and histopathological data. Measurements were done in 13 dogs in the control stage, in 11 dogs in the SMI stage, and in 7 dogs in the TMI stage. Because of a large infarct created by the procedure, two dogs did not survive in the SMI stage and four dogs in the TMI stage. The absolute value of peak systolic left ventricular pressure and peak positive and negative dP/d*t* decreased gradually with the advancement of the stage. However, heart rate showed no significant changes. Both positive and negative dP/d*t* significantly increased in response to dobutamine administration (Table 1 and Fig. 4).

The degree of infarct extension was assessed at 14 sites from 4 dogs after the SMI stage and at 20 sites from 7 dogs after the TMI stage. The infarct extension index was 24.9 ± 7.8% for the SMI stage and 76.1 ± 9.9% for the TMI stage. Typical examples of the histopathological findings for both subendocardial and transmural infarcts are shown in Fig. 3.

Strain value in each stage. Myocardial strain was obtained at 25 segments in the control stage, at 20 segments in the SMI stage, and 11 segments in the TMI stage. Figure 5 shows representative TMSPs in each stage. In the control stage, myocardial strain was highest in the subendocardium and declined linearly toward the subepicardium. After DSE, TMSP

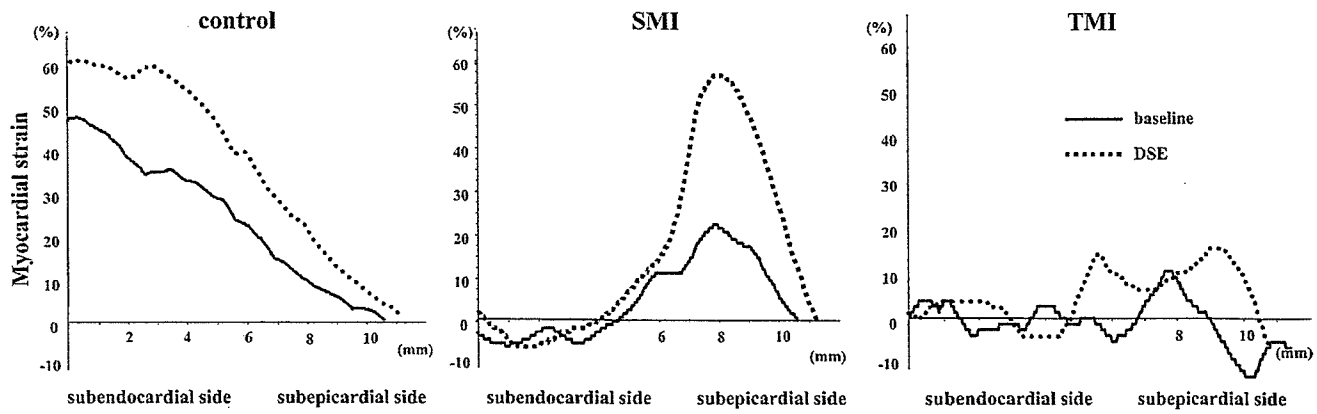

Fig. 5. Transmural myocardial strain profile before (solid lines) and after (dashed lines) dobutamine administration in each stage. *Left*: control stage. The profile was highest at the subendocardium and lowest at the subepicardium. With dobutamine administration, overall transmural myocardial strain increased. *Middle*: SMI stage. Myocardial strain at the subendocardium significantly decreased. With dobutamine administration, myocardial strain at the subepicardium showed a significant increase. *Right*: TMI stage. Overall transmural myocardial strain decreased at the baseline. Even after dobutamine administration, myocardial strain showed no significant increase.

Table 2. *Subendocardial and subepicardial strain in control, SMI, and TMI stages*

	Baseline			DSE		
	Control (n = 25)	SMI (n = 20)	TMI (n = 11)	Control	SMI	TMI
Endo strain	53.6±17.1*†‡	0.8±8.8	−3.9±5.6	73.3±21.8†‡	1.3±7.0	−1.9±6.0
Epi strain	23.9±6.1*†‡	12.4±7.3*†	−1.0±7.8	26.3±6.4†	27.1±8.8†	−0.7±8.3

Data are presented as means ± SD; n, no. of dogs. Endo strain, subendocardial strain; Epi strain, subepicardial strain. $P < 0.05$ vs. DSE values (*), vs. SMI values (‡), and vs. TMI values (†).

was uniformly uplifted, indicating the enhancement of contractility. In the SMI stage, subendocardial strain was almost zero before and after dobutamine challenge. In contrast, subepicardial strain increased after dobutamine, suggesting the presence of myocardial viability in the subepicardium. In the TMI stage, TMSP was almost flat before and after DSE, showing loss of myocardial viability through whole layers (Table 2).

Figure 6 shows changes in the subendocardial and subepicardial mean strain. Strain in the subendocardial half-layer was lower in the SMI and TMI stages than in the control stage (53.6 ± 17.1 vs. 0.8 ± 8.8 and −3.9 ± 5.6%, both $P < 0.001$).

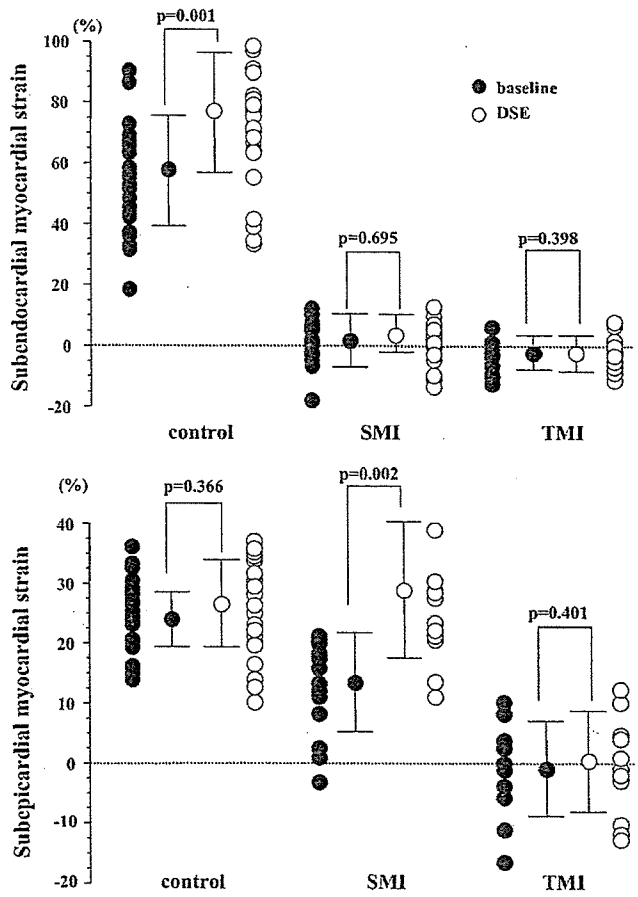

Fig. 6. Strain value in each layer. *Top*: subendocardial strain before (●) and after (○) dobutamine administration. Strain value in the subendocardial half-layer in the control stage increased with dobutamine, whereas that in the SMI and TMI stages showed no significant increase. *Bottom*: subepicardial strain before (●) and after (○) dobutamine administration. Strain value in the subepicardial half-layer in the SMI stage showed a significant increase. It showed no significant increase in the TMI stage.

There were no significant differences in the subendocardial strain between the SMI and TMI stages [P = not significant (NS)]. Strain in the subepicardial half-layer was lower in the TMI stage (−1.0 ± 7.8%) than that in the SMI stage (12.4 ± 7.3%, $P < 0.001$) and that in the control stage (23.9 ± 6.1%, $P < 0.001$).

Subendocardial strain in the control stage increased with DSE (53.6 ± 17.1 vs. 73.3 ± 21.8%, $P < 0.001$), whereas that in the SMI (0.8 ± 8.8 vs. 1.3 ± 7.0%, P = NS) and in the TMI stage (−3.9 ± 5.6 vs. −1.9 ± 6.0%, P = NS) showed no significant increase. Subepicardial strain in the control stage (23.9 ± 6.1 vs. 26.3 ± 6.4%, $P < 0.05$) and in the SMI stage (12.4 ± 7.3 vs. 27.1 ± 8.8%, $P < 0.005$) increased with DSE. It did not increase after DSE in the TMI stage (−1.0 ± 7.8 vs. −0.7 ± 8.3%, P = NS). Subepicardial strain after DSE showed no significant differences between the control and SMI stages (P = NS). These results showed that myocardial viability in the subepicardium was preserved in the SMI stage, whereas that in the TMI stage was lost.

DISCUSSION

In the present study, we analyzed the transmural distribution of viable muscle in myocardial infarction using echocardiography. Contraction in the subendocardium was lost and did not increase with dobutamine in either subendocardial infarction or transmural infarction models. On the other hand, subepicardial contraction was increased in subendocardial infarction but not in transmural infarction. These results showed that, with TMSP, we could quantify the transmural distribution of myocardial strain and identify the transmural differences in a local inotropic reserve in the viable and infarcted myocardium. The TMSP with DSE was useful to estimate the heterogeneity of transmural myocardial viability in SMI and TMI.

Transmural heterogeneity of myocardial viability. The left ventricular myocardium demonstrates transmural heterogeneity of strain distribution. It has been reported that, under normal circumstances, the subendocardial myocardium receives more blood flow and consumes more oxygen than the subepicardial one (20, 28, 35). Moreover, there is a transmural gradient of contractile function in the left ventricular wall, with greatest amount of thickening occurring in the subendocardial myocardium (6, 25). Clinically, these results were noninvasively confirmed in healthy subjects with tissue Doppler tracking technique (31). In the present study, strain value in the subendocardial layer was greater than that in the subepicardial layer in the control stage, being consistent with those of previous experimental and clinical studies. The linear decline pattern in TMSP was not observed in myocardial infarction. TMSP would potentially be useful for more detailed and innovative

evaluations of transmural myocardial function experimentally and clinically.

Effect of ischemia and dobutamine on transmural heterogeneity. After coronary artery occlusion, myocardial necrosis begins first in the endocardium and then progresses toward the epicardium with an increase in the occlusion time (8, 13). In our present study, we confirmed histologically that the SMI stage induced subendocardial infarction and the TMI stage induced transmural myocardial infarction. We observed continuous progression of myocardial dysfunction from the subendocardium to the subepicardium in myocardial infarction using echocardiography.

In acute animal models of reversible postischemic dysfunction and myocardial infarction, improved wall thickening during inotropic stimulation accurately differentiated reversible from fixed dysfunction and provided a better early assessment of viability than assessment of resting function alone (18). In clinical studies, contractile reserve by low-dose dobutamine was an independent predictor of functional recovery for myocardial infarction, which was superior to the other clinical criteria (23). In this experimental subendocardial infarction model, subendocardial strain showed no significant increase in response to inotropic stimulation, whereas subepicardial strain increased, indicating that the subepicardial myocardium was still viable. In the transmurally infarcted myocardium, myocardial strain of both subendocardium and subepicardium did not show significant increase. Therefore, the present method using TMSP and DSE is useful to visualize and quantify the contractile reserve and viability of both the subendocardium and the subepicardium.

Clinical implications. Because the prognosis of patients with subendocardial infarction is better than that with transmural infarction, assessment of the transmurality of myocardial necrosis and ischemia is an important clinical issue for patients with acute myocardial infarction or with chronic myocardial ischemia (22, 27). However, it has been difficult to make a diagnosis of subendocardial infarction by two-dimensional echocardiography. Some previous studies have shown that strain rate or strain echocardiography was useful to differentiate subendocardial infarction from transmural infarction (2, 34). We also obtained similar results using a new method of visualizing transmural myocardial strain distribution. Because the transmurality of necrosis is an important determinant of ultimate infarct size, its knowledge would be helpful in making therapeutic decisions for myocardial infarction (16, 34). Thus it is clinically helpful that we can quantify the transmural myocardial viability and necrosis extent. Furthermore, we could estimate the myocardial viability of each layer with DSE, enabling us to diagnose the stunned myocardium and predict myocardial functional recovery after myocardial infarction.

The present imaging system can be applied for the clinical evaluation of the various heart diseases characterized by subendocardial myocardial dysfunction such as anthracycline cardiotoxicity, syndrome X, hypertrophic cardiomyopathy, and dilated cardiomyopathy (14, 19, 21).

Study limitations. There was a possibility that some dogs in the subendocardial infarction models might develop transmural infarction. However, the 90-min ischemic period chosen for the subendocardial infarction models was similar to the previous studies, and it did result in subendocardial infarction (8, 10). In the present study, we showed histological evidence of subendocardial infarction after the SMI stage in parts of dogs. Furthermore, the difference in strain between the subendocardial and transmural infarction models was very prominent and consistent in each dog in the present study. These suggested that dogs after the SMI stage developed myocardial infarct almost only in the subendocardial layer.

We did not validate myocardial strain values using other methods, such as sonomicrometry. However, sonomicrometry is not always suitable to assess transmural distribution of myocardial strain, as shown in Fig. 5. We believe our measurement should be accurate because the displacement data obtained by our method were shown to be accurate (3, 21).

In conclusion, the quantitative analysis of transmural myocardial strain distribution could assess transmural differences in local inotropic reserve within the viable and infracted myocardium. In subendocardial infarction, the subepicardial myocardial strain showed an increase in contraction with dobutamine. However, in transmural infarction, this increase was lost. Assessment of transmural strain profile using tissue strain imaging was useful to quantify transmural distribution of the viable myocardium in SMI and TMI.

ACKNOWLEDGMENTS

We thank Yasuhiko Abe, Ryoichi Kanda, and Toshiba Corporation for providing research software assistance.

GRANTS

This work was partly supported by a Research Grant from the Ministry of Health, Labor and Welfare, Japan.

REFERENCES

1. **Chen X, Nakatani S, Hasegawa T, Maruo T, Kanzaki H, Miyatake K.** Effect of left ventricular systolic pressure on myocardial strain demonstrated by transmural myocardial strain profile. *Echocardiography* 23: 77–78, 2006.
2. **Derumeaux G, Loufoua J, Pontier G, Cribier A, Ovize M.** Tissue Doppler imaging differentiates transmural from nontransmural acute myocardial infarction after reperfusion therapy. *Circulation* 103: 589–596, 2001.
3. **Dohi K, Pinsky MR, Kanzaki H, Severyn D, Gorcsan J 3rd.** Effects of radial left ventricular dyssynchrony on cardiac performance using quantitative tissue Doppler radial strain imaging. *J Am Soc Echocardiogr* 19: 475–482, 2006.
4. **Edvardsen T, Gerber BL, Garot J, Bluemke DA, Lima JA, Smiseth OA.** Quantitative assessment of intrinsic regional myocardial deformation by Doppler strain rate echocardiography in humans: validation against three-dimensional tagged magnetic resonance imaging. *Circulation* 106: 50–56, 2002.
5. **Gallagher KP, Matsuzaki M, Koziol JA, Kemper WS, Ross J Jr.** Regional myocardial perfusion and wall thickening during ischemia in conscious dogs. *Am J Physiol Heart Circ Physiol* 247: H727–H738, 1984.
6. **Hartley CJ, Latson LA, Michael LH, Seidel CL, Lewis RM, Entman ML.** Doppler measurement of myocardial thickening with a single epicardial transducer. *Am J Physiol Heart Circ Physiol* 245: H1066–H1072, 1983.
7. **He KL, Dickstein M, Sabbah HN, Yi GH, Gu A, Maurer M, Wei CM, Wang J, Burkhoff D.** Mechanisms of heart failure with well preserved ejection fraction in dogs following limited coronary microembolization. *Cardiovasc Res* 64: 72–83, 2004.
8. **Homans DC, Pavek T, Laxson DD, Bache RJ.** Recovery of transmural and subepicardial wall thickening after subendocardial infarction. *J Am Coll Cardiol* 24: 1109–1116, 1994.
9. **Jamal F, Strotmann J, Weidemann F, Kukulski T, D'hooge J, Bijnens B, Van de Werf F, De Scheerder I, Sutherland GR.** Noninvasive quantification of the contractile reserve of stunned myocardium by ultrasonic strain rate and strain. *Circulation* 104: 1059–1065, 2001.
10. **Kim WG, Shin YC, Hwang SW, Lee C, Na CY.** Comparison of myocardial infarction with sequential ligation of the left anterior descend-

ing artery and its diagonal branch in dogs and sheep. *Int J Artif Organs* 26: 351–357, 2003.

11. **Kukulski T, Jamal F, Herbots L, D'hooge J, Bijnens B, Hatle L, De Scheerder I, Sutherland GR.** Identification of acutely ischemic myocardium using ultrasonic strain measurements. A clinical study in patients undergoing coronary angioplasty. *J Am Coll Cardiol* 41: 810–819, 2003.
12. **Lavine SJ, Prcevski P, Held AC, Johnson V.** Experimental model of chronic global left ventricular dysfunction secondary to left coronary microembolization. *J Am Coll Cardiol* 18: 1794–1803, 1991.
13. **Lowe JE, Cummings RG, Adams DH, Hull-Ryde EA.** Evidence that ischemic cell death begins in the subendocardium independent of variations in collateral flow or wall tension. *Circulation* 68: 190–202, 1983.
14. **Maier SE, Fischer SE, McKinnon GC, Hess OM, Krayenbuehl HP, Boesiger P.** Evaluation of left ventricular segmental wall motion in hypertrophic cardiomyopathy with myocardial tagging. *Circulation* 86: 1919–1928, 1992.
15. **Malyar NM, Lerman LO, Gossl M, Beighley PE, Ritman EL.** Relation of nonperfused myocardial volume and surface area to left ventricular performance in coronary microembolization. *Circulation* 110: 1946–1952, 2004.
16. **Mann DL, Gillam LD, Mich R, Foale R, Newell JB, Weyman AE.** Functional relation between infarct thickness and regional systolic function in the acutely and subacutely infarcted canine left ventricle. *J Am Coll Cardiol* 14: 481–488, 1989.
17. **Matre K, Fannelop T, Dahle GO, Heimdal A, Grong K.** Radial strain gradient across the normal myocardial wall in open-chest pigs measured with Doppler strain rate imaging. *J Am Soc Echocardiogr* 18: 1066–1073, 2005.
18. **Mercier JC, Lando U, Kanmatsuse K, Ninomiya K, Meerbaum S, Fishbein MC, Swan HJ, Ganz W.** Divergent effects of inotropic stimulation on the ischemic and severely depressed reperfused myocardium. *Circulation* 66: 397–400, 1982.
19. **Mortensen SA, Olsen HS, Baandrup U.** Chronic anthracycline cardiotoxicity: haemodynamic and histopathological manifestations suggesting a restrictive endomyocardial disease. *Br Heart J* 55: 274–282, 1986.
20. **Oh BH, Volpini M, Kambayashi M, Murata K, Rockman HA, Kassab GS, Ross J Jr.** Myocardial function and transmural blood flow during coronary venous retroperfusion in pigs. *Circulation* 86: 1265–1279, 1992.
21. **Panting JR, Gatehouse PD, Yang GZ, Grothues F, Firmin DN, Collins P, Pennell DJ.** Abnormal subendocardial perfusion in cardiac syndrome X detected by cardiovascular magnetic resonance imaging. *N Engl J Med* 346: 1948–1953, 2002.
22. **Picano E, Sicari R, Landi P, Cortigiani L, Bigi R, Coletta C, Galati A, Heyman J, Mattioli R, Previtali M, Mathias W Jr, Dodi C, Minardi G, Lowenstein J, Seveso G, Pingitore A, Salustri A, Raciti M.** Prognostic value of myocardial viability in medically treated patients with global left ventricular dysfunction early after an acute uncomplicated myocardial infarction: a dobutamine stress echocardiographic study. *Circulation* 98: 1078–1084, 1998.
23. **Pierard LA, De Landsheere CM, Berthe C, Rigo P, Kulbertus HE.** Identification of viable myocardium by echocardiography during dobutamine infusion in patients with myocardial infarction after thrombolytic therapy: comparison with positron emission tomography. *J Am Coll Cardiol* 15: 1021–1031, 1990.
24. **Pislaru C, Bruce CJ, Anagnostopoulos PC, Allen JL, Seward JB, Pellikka PA, Ritman EL, Greenleaf JF.** Ultrasound strain imaging of altered myocardial stiffness: stunned versus infarcted reperfused myocardium. *Circulation* 109: 2905–2910, 2004.
25. **Sabbah HN, Marzilli M, Stein PD.** The relative role of subendocardium and subepicardium in left ventricular mechanics. *Am J Physiol Heart Circ Physiol* 240: H920–H926, 1981.
26. **Sade LE, Severyn DA, Kanzaki H, Dohi K, Gorcsan J 3rd.** Second-generation tissue Doppler with angle-corrected color-coded wall displacement for quantitative assessment of regional left ventricular function. *Am J Cardiol* 92: 554–560, 2003.
27. **Sawada S, Bapat A, Vaz D, Weksler J, Fineberg N, Greene A, Gradus-Pizlo I, Feigenbaum H.** Incremental value of myocardial viability for prediction of long-term prognosis in surgically revascularized patients with left ventricular dysfunction. *J Am Coll Cardiol* 42: 2099–2105, 2003.
28. **Sjoquist PO, Duker G, Almgren O.** Distribution of the collateral blood flow at the lateral border of the ischemic myocardium after acute coronary occlusion in the pig and the dog. *Basic Res Cardiol* 79: 164–175, 1984.
29. **Skulstad H, Urheim S, Edvardsen T, Andersen K, Lyseggen E, Vartdal T, Ihlen H, Smiseth OA.** Grading of myocardial dysfunction by tissue Doppler echocardiography: a comparison between velocity, displacement, and strain imaging in acute ischemia. *J Am Coll Cardiol* 47: 1672–1682, 2006.
30. **Tanaka N, Tone T, Ono S, Tomochika Y, Murata K, Kawagishi T, Yamazaki N, Matsuzaki M.** Predominant inner-half wall thickening of left ventricle is attenuated in dilated cardiomyopathy: an application of tissue Doppler tracking technique. *J Am Soc Echocardiogr* 14: 97–103, 2001.
31. **Torry RJ, Myers JH, Adler AL, Liut CL, Gallagher KP.** Effects of nontransmural ischemia on inner and outer wall thickening in the canine left ventricle. *Am Heart J* 122: 1292–1299, 1991.
32. **Uematsu M, Miyatake K, Tanaka N, Matsuda H, Sano A, Yamazaki N, Hirama M, Yamagishi M.** Myocardial velocity gradient as a new indicator of regional left ventricular contraction: detection by a two-dimensional tissue Doppler imaging technique. *J Am Coll Cardiol* 26: 217–223, 1995.
33. **Urheim S, Edvardsen T, Torp H, Angelsen B, Smiseth OA.** Myocardial strain by Doppler echocardiography. Validation of a new method to quantify regional myocardial function. *Circulation* 102: 1158–1164, 2000.
34. **Weidemann F, Dommke C, Bijnens B, Claus P, D'hooge J, Mertens P, Verbeken E, Maes A, Van de Werf F, De Scheerder I, Sutherland GR.** Defining the transmurality of a chronic myocardial infarction by ultrasonic strain-rate imaging: implications for identifying intramural viability: an experimental study. *Circulation* 107: 883–888, 2003.
35. **Weiss HR, Neubauer JA, Lipp JA, Sinha AK.** Quantitative determination of regional oxygen consumption in the dog heart. *Circ Res* 42: 394–401, 1978.
36. **Williams RI, Payne N, Phillips T, D'hooge J, Fraser AG.** Strain rate imaging after dynamic stress provides objective evidence of persistent regional myocardial dysfunction in ischaemic myocardium: regional stunning identified? *Heart* 91: 152–160, 2005.

Sustained Elevation of Serum Cortisol Level Causes Sensitization of Coronary Vasoconstricting Responses in Pigs In Vivo

A Possible Link Between Stress and Coronary Vasospasm

Takatoshi Hizume, Keiko Morikawa, Aya Takaki, Kohtaro Abe, Kenji Sunagawa, Mutsuki Amano, Kozo Kaibuchi, Chiharu Kubo, Hiroaki Shimokawa

Abstract—Vasospastic angina is induced by stress, for which cortisol secreted by activated hypothalamic/pituitary/adrenal axis may play an important role. However, direct evidence for this notion is still lacking. In this study, we examined whether sustained elevation of serum cortisol level sensitizes coronary vasoconstricting responses in pigs in vivo and, if so, whether Rho-kinase, which we found is a key molecule of coronary vasospasm, is involved. Oral administration of cortisol (20 mg/kg per day) increased its serum level to that seen in restraint stress in pigs. Thus, we examined coronary vasomotor responses in the following 4 groups: (1) control (without cortisol); (2) cortisol (20 mg/kg per day, PO) for 9 days; (3) cortisol plus RU38486 (a glucocorticoids receptor antagonist, 10 mg/kg per day, PO) for 9 days; and (4) cortisol for 9 days followed by 6-week withdrawal. Coronary angiography showed that intracoronary serotonin caused coronary hyperconstriction and reduction in coronary blood flow associated with ischemic ECG changes (coronary vasospasm) in only the cortisol group. All of these responses were abolished by hydroxyfasudil, a specific Rho-kinase inhibitor, in vivo. Organ chamber experiments demonstrated that serotonin concentration-dependently caused hypercontractions of coronary vascular smooth muscle associated with Rho-kinase activation (as evidenced by the enhanced phosphorylation of myosin binding subunit, a substrate of Rho-kinase) in only the cortisol group. All of these responses were again inhibited by hydroxyfasudil in vitro. These results indicate that sustained elevation of serum cortisol level sensitizes coronary vasoconstricting responses through Rho-kinase activation, suggesting the link between stress and coronary vasospasm. (*Circ Res.* **2006;99:767-775.**)

Key Words: Rho-kinase ■ coronary vasospasm ■ cortisol ■ myocardial ischemia ■ stress

Physical and/or mental stress induces ischemic attacks in patients with coronary artery disease (CAD). Recent studies have demonstrated that psychological factors are involved in the pathogenesis of CAD[1–4] and that stress could induce coronary vasospasm and myocardial ischemia.[5–7] Indeed, stress test is clinically used to induce vasospastic angina.[8] However, it remains to be examined what component(s) and mechanism(s) of stress are responsible for coronary vasospasm. These points are important to develop an effective therapy to prevent stress-induced myocardial ischemia and sudden death.

Cortisol is among the major stress hormones and is secreted by the activated hypothalamic/pituitary/adrenal axis in physical and/or mental stress.[9–12] Cortisol also could cause endothelial and baroreflex dysfunction.[9,13–15] Short-term oral administration of a high-dose of cortisol impairs endothelial function even in healthy subjects.[14]

Rho-kinase/ROK/ROCK, one of the effectors of the small GTPase Rho, plays an important role in vascular smooth muscle cell (VSMC) contraction.[16–20] In a series of experimental and clinical studies, we have demonstrated that enhanced Rho-kinase activity plays a central role for coronary vasospasm in both animals and humans.[16–20] However, it remains to be examined whether Rho-kinase also is involved in the stress-induced coronary vasospasm.

In the present study, we thus examined whether sustained elevation of serum cortisol level sensitizes coronary vasoconstricting responses in pigs in vivo and, if so, whether Rho-kinase is involved in the molecular mechanism for the sensitization.

Materials and Methods

All procedures were approved by the Institutional Animal Care and Use Committee and were conducted according to the institutional guidelines of Kyushu University.

Original received June 4, 2006; revision received August 11, 2006; accepted August 24, 2006.

From the Departments of Cardiovascular Medicine (T.H., K.M., A.T., K.A., K.S., H.S.) and Psychosomatic Medicine (T.H., C.K.), Kyushu University Graduate School of Medical Sciences, Fukuoka; Department of Cell Pharmacology (M.A., K.K.), Nagoya University Graduate School of Medicine; Department of Cardiovascular Medicine (A.T., H.S.), Tohoku University Graduate School of Medicine, Sendai; and Japan Science and Technology Agency (H.S.), Core Research for Evolutional Science and Technology, Tokyo.

Correspondence to Hiroaki Shimokawa, MD, PhD, Professor and Chairman, Department of Cardiovascular Medicine, Tohoku University Graduate School of Medicine, Seiryo-machi, Aoba-ku, Sendai 980-8574, Japan. E-mail shimo@cardio.med.tohoku.ac.jp

Circulation Research **is available at http://circres.ahajournals.org** **DOI: 10.1161/01.RES.0000244093.69985.2f**

Protocols

A total of 74 male domestic pigs (3 to 5 months, 25 to 30 kg) were used (Kyudo, Tosu, Japan).

Experiment 1: Determination of the Dose of Cortisol

Animals were implanted with a catheter in the jugular vein 5 days before the restraint stress test and were divided into the control, cortisol, and restraint stress groups (n=6 each). The cortisol group was given daily 20 mg/kg of cortisol in drinking water, whereas the other 2 groups were without any medication. The restraint stress group was tethered with a neck chain attached to the small pen (40×100×80 cm) from 8:00 AM to 8:00 PM, and were released from 8:00 PM to 8:00 AM the next morning.[21,22] Blood samples were collected at 3:00 AM, 9:00 AM, 3:00 PM, and 9:00 PM over 24 hours during the experiment. The hourly averages of area under the curve (AUC) of serum cortisol level were evaluated.[23]

Experiment 2: Coronary Vasomotor Responses to Chronic Cortisol Treatment

Pigs were used for coronary angiography (CAG) study (n=26), organ chamber experiments (n=26), and Western blot analysis (n=19). They were housed individually under a controlled room temperature. For CAG study, the animals were divided into the following 4 groups: (1) control group (n=8); (2) cortisol group treated with oral administration of cortisol (20 mg/kg per day) from day 1 to 7 and 9 and 10 (n=8); (3) RU group treated with cortisol (20 mg/kg per day) plus RU38486 (10 mg/kg per day), a glucocorticoid receptor antagonist,[24] on the same schedule as in the cortisol group (n=5); and (4) withdrawal group, which was treated as in the cortisol group, followed by withdrawal of cortisol from day 11 to 55. In the control, cortisol, and RU groups, CAG was performed on day 8, whereas it was performed on both day 8 and 52 in the withdrawal group (n=5). Organ chamber experiment was performed on day 11 in the control, cortisol, and RU groups (n=5 to 8) and on day 55 in the withdrawal group (n=5). All animals were fasted without any medication for 24 hours before the experiments.

Coronary Angiography

Animals were anesthetized with ketamine hydrochloride (15 mg/kg, IM) and pentobarbital (20 mg/kg, IV). They were then intubated and mechanically ventilated with room air. After systemic heparinization (5000 U/body), a preshaped 8F Judkins catheter was inserted through the carotid artery. CAG of the left coronary artery (LCA) was performed in a left oblique view with the cineangiography system (Toshiba Medical, Tokyo, Japan).[19,25,26] ECGs (leads I, II, and III) and arterial pressure were continuously monitored (Nihon Kohden, Tokyo, Japan).[19,25,26] Blood chemistry values (Na, K, Cl, blood urea nitrogen [BUN], creatinine [Cr], glutamate oxaloacetic transaminase [GOT], glutamate pyruvate transaminase [GPT], lactate dehydrogenase [LDH], creatine phosphokinase [CPK]) were also measured. End-diastolic frames were selected to measure coronary diameters. The measurement was made in a blind manner at the left anterior descending coronary artery (LAD), at both the large (just proximal to the first diagonal branch) and small (distal portion of the branch with a baseline diameter of ≈500 μm) coronary arteries.[19,25,26]

Protocols of CAG Study

First, CAG was performed under control conditions. Second, coronary vasomotor responses to serotonin (10 and 100 μg/kg, IC) were examined.[16,19,25,26] Serotonin induces coronary vasospasm that is similar to spontaneous spasm in humans compared with acetylcholine.[27] Third, endothelium-dependent vasodilating responses to bradykinin (0.1 μg/kg, IC) were examined.[25] Fourth, vasoconstricting responses to serotonin (100 μg/kg, IC) were examined after intracoronary infusion of hydroxyfasudil (30 and 100 μg/kg/min for 3 minutes), a specific Rho-kinase inhibitor.[26] Fifth, vasodilating responses to bradykinin (0.1 μg/kg, IC) were examined after intracoronary infusion of N^G-monomethyl-L-arginine (L-NMMA, 1 mg/kg for 10 minutes).[25] Finally, endothelium-independent vasodilating responses to nitroglycerin (10 μg/kg, IC) were examined.[25] CAG was performed 2 minutes after intracoronary administration of serotonin, bradykinin, or nitroglycerin, when the vasodilator or vasoconstrictor effect of each agent peaked.[19,25,26] Each protocol was performed with an interval of 20 to 30 minutes after the confirmation of disappearance of a drug effect by CAG and hemodynamic measurements. Each dose of drugs was diluted with 3 mL of physiological saline, except hydroxyfasudil, which was diluted with 3 mL of distillated water. The degree of coronary vasoconstricting response was expressed as percent change in luminal diameter and blood flow from the baseline values.[19,25,26]

Coronary Blood Flow Measurement

Coronary blood flow velocity was measured by a Doppler guide wire (FloWire, 12 MHz, Cardiometrics, Mountain View, Calif) at the same time with CAG. A 0.014-inch tip Doppler guide wire was advanced via the guiding catheter into the proximal LAD. The position of the Doppler guide wire was kept constant throughout the study. The time average of the spectral peak velocity (APV) was used for mean coronary blood flow velocity.[28] Coronary blood flow was calculated by multiplying a half APV by calculated coronary sectional area at the tip of the Doppler guide wire on the corresponding angiogram.[28]

Organ Chamber Experiments

Three days after the CAG study, animals were sedated with ketamine hydrochloride (15 mg/kg, IM), euphonized with a lethal dose of sodium pentobarbital (40 mg/kg, IV), and then the heart was excised. Epicardial and distal small (≈200 to 250 μm in inner diameter) right coronary arteries (RCA) were carefully dissected and cleaned of any perivascular connective tissue. We used RCA for organ chamber experiments to avoid any influence of CAG on LCA. We have previously confirmed that there are no differences in vascular responses (both in vivo and in vitro) between RCA and LCA,[29] which we also confirmed in the present study (Figure I in the online data supplement, available at http://circres.ahajournals.org). Epicardial RCA were cut into 8 rings (≈4 mm in length),[16,17,25,26] whereas distal small RCA into 8 rings (≈1 mm in length).[30,31] In 4 rings of both-sized arteries, the endothelium was removed by gentle rubbing of the luminal surface with a cotton swab.[17,25,30]

The rings were fixed vertically between hooks in an organ bath containing Krebs–Henseleit solution at 37°C with a mixture of 95% O_2/5% CO_2 and isometric tension was measured with force transducers (Nihon Kohden Inc). KCl solution (62 mmol/L) was applied every 15 minutes until the amplitude of contraction reached a constant value. The developed tension was expressed as a percentage of that attained in the last precontraction with 62 mmol/L KCl.[17,25,30] The presence and absence of the endothelium was confirmed by the presence and absence of relaxation to bradykinin (10^{-7} mol/L) during a contraction evoked by KCl, respectively.[25]

The direct VSMC vasocontracting effect of serotonin (10^{-9} to 10^{-5} mol/L) was evaluated in rings without endothelium.[17,26] The acute inhibitory effect of hydroxyfasudil on serotonin-induced VSMC contraction was examined after equilibration with hydroxyfasudil (10^{-6} and 3×10^{-6} mol/L, for 30 minutes) separately in different rings without endothelium.[17,26] Endothelium-dependent relaxations to bradykinin (10^{-11} to 10^{-6} mol/L) were examined in rings with endothelium during a contraction evoked by prostaglandin (PG) $F_{2\alpha}$ (2×10^{-6} mol/L). The extent of contraction in response to $PGF_{2\alpha}$ was adjusted to 50% to 70% of that induced by 62 mmol/L KCl.[25,30,31] The contribution of vasodilator PGs, nitric oxide (NO), and endothelium-derived hyperpolarizing factor (EDHF) to endothelium-dependent relaxations to bradykinin was evaluated by determining the inhibitory effect of indomethacin (10^{-5} mol/L), N^{ω}-nitro-L-arginine (L-NNA, 10^{-4} mol/L), and charybdotoxin (an inhibitor of large and intermediate-conductance KCa channels, 100 nmol/L) plus apamin (an inhibitor of small conductance KCa channels, 1 μmol/L), respectively.[30,31] Endothelium-independent relaxations to sodium nitroprusside (SNP) (10^{-10} to 10^{-5} mol/L) also were examined in rings without endothelium.

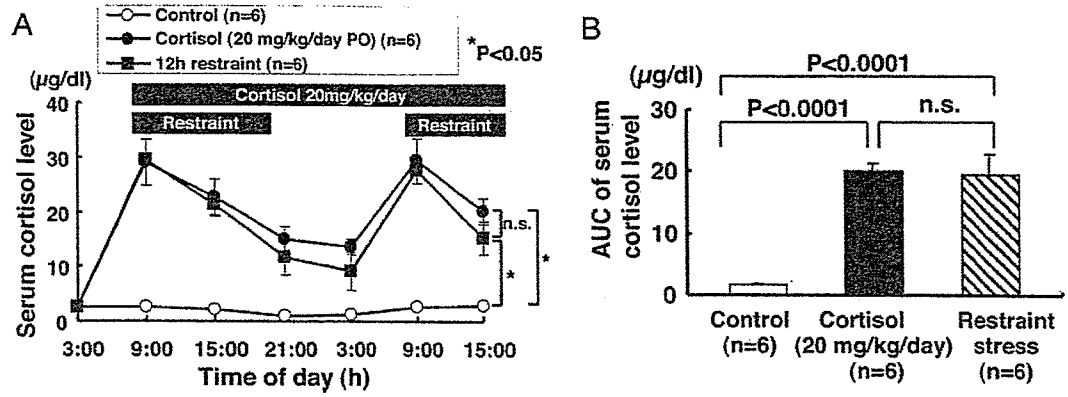

Figure 1. Daily profile (A) and areas under the curve (AUC) (B) of serum cortisol level during restraint stress and oral administration of the hormone. The oral administration of cortisol significantly increased serum cortisol level, equivalent to that in restraint stress. Results are expressed as mean±SEM. n.s. indicates not significant.

To evaluate the acute effect of cortisol on coronary vasomotor responses, organ chamber experiments were also performed in rings with or without endothelium from normal coronary arteries in the absence and presence of cortisol (10 and 30 μg/dL for 60 minutes and 30 μg/dL for 120 minutes).

Histopathology

LCA were perfused via constant-pressure perfusion system (120 cm H_2O) with saline (1000 mL) and subsequently with 5% formaldehyde (1000 mL).[19,32] After fixation, LAD was cut transversely, dehydrated, embedded in paraffin, and cut into 5-μm-thick slices. These segments were stained with hematoxylin/eosin and van Gieson's elastic staining for histological analysis.

Western Blot Analysis for Rho-Kinase Activity

Rho-kinase activity can be evaluated by the extent of phosphorylation of myosin-binding subunit (MBS) of myosin phosphatase, a substrate of Rho-kinase.[16,32–34] The regions containing MBS were visualized by ECL Western blotting luminal reagent (Santa Cruz Biotechnology, Santa Cruz, Calif).[16,17,32] Isolated RCA rings without endothelium were subjected to SDS-PAGE immunoblot analysis when serotonin-induced (10^{-6} mol/L) contraction reached a maximum.[16,17,32] Rho-kinase activity is expressed by the extent of MBS phosphorylation when normalized to total MBS.

Statistical Analysis

Results are expressed as mean±SEM. χ^2 test was used for comparison of ECG ST-segment changes. Results of CAG and blood flow were analyzed by 2-way ANOVA followed by Bonferroni test for multiple comparisons. Serum cortisol levels under control condition and during oral administration of cortisol and restraint stress, AUC of serum cortisol level, and the results of organ chamber experiments were analyzed by 2-way ANOVA, followed by Scheffe test for multiple comparisons. The results of Western blot analysis were analyzed by Dunnet test. A value of $P<0.05$ was considered to be statistically significant.

Results

Daily Profile of Serum Cortisol Level During Restraint Stress and Oral Administration

Daily profile (Figure 1A) and AUC (Figure 1B) of serum cortisol levels were comparable between restraint stress and oral administration of the hormone.

Coronary Vascular Responses to Serotonin In Vivo

Among the control, cortisol, and RU groups, hemodynamic variables (heart rate and blood pressure) (supplemental Table I) and blood chemistry values (data not shown) were comparable. Because cortisol was stopped 24 hours before the CAG experiment, the serum cortisol level (μg/dL) was comparable among the 3 groups (2.4±0.8 in the control, 1.9±0.5 in the cortisol, and 2.1±0.7 in the RU group, n=5 each).

There was no significant difference in baseline coronary diameter among the 3 groups (supplemental Table II). A low dose of serotonin (10 μg/kg, IC) caused mild coronary vasodilatation without any significant ECG changes in the control (Figure 2A through 2D) and RU (Figure 2I through 2L) groups but caused intense and diffuse vasoconstriction, especially at small coronary arteries, with ischemic ST changes in the cortisol group (ST elevation in 3/5 and ST depression in 1/5) (Figure 2E through 2H). By contrast, a high dose of serotonin (100 μg/kg, IC) caused coronary vasoconstriction in large (Figure 3G) and small (Figure 3H) arteries in all the 3 groups; however, the extent of the vasoconstriction was most prominent in the cortisol group, especially at small coronary arteries (Figure 3G and 3H). Intracoronary pretreatment with hydroxyfasudil dose-dependently suppressed the serotonin-induced vasoconstrictions in all the 3 groups (Figure 3).

Coronary blood flow was slightly increased in response to a low dose of serotonin but was decreased to a high dose of serotonin in the control and RU groups (Figure 3I). By contrast, in the cortisol group, coronary blood flow was decreased in response to both doses of serotonin, which was again dose-dependently inhibited and was converted to an increase in the flow by hydroxyfasudil, as seen in other 2 groups (Figure 3I).

Coronary Endothelial Vasodilator Function In Vivo

Bradykinin (0.1 μg/kg, IC) caused mild coronary vasodilatation in both-sized arteries and an increase in coronary blood flow in all the 3 groups (Figure 4). Pretreatment with intracoronary L-NMMA tended to inhibit the bradykinin-induced coronary vasodilatation in all groups, whereas nitroglycerin (10 μg/kg, IC) caused a comparable extent of coronary vasodilatation and increase in coronary blood flow in all groups (Figure 4).

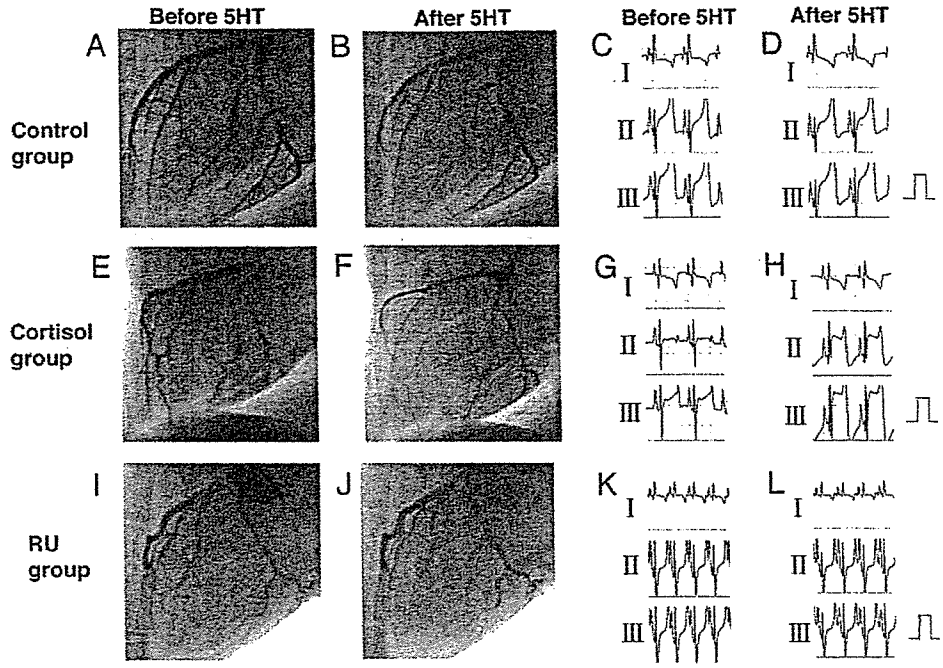

Figure 2. Coronary angiograms and ECG before and after a low dose of serotonin (5HT) (10 μg/kg, IC). Serotonin induced mild coronary vasodilatation with no ischemic ECG changes in the control (A through D) and RU (I through L) groups but induced diffuse and intense coronary vasoconstriction with ischemic ST changes in the cortisol group (E through H). Calibration on ECG, 1 mV.

Effect of Withdrawal of Long-Term Treatment With Cortisol

In the withdrawal group, there was no significant difference in basal coronary diameters as compared with other 3 groups (supplemental Table I) or between day 8 (before cessation of the cortisol treatment) and day 52 (6 weeks after withdrawal) (supplemental Table III). On day 8, intracoronary serotonin again caused intense and diffuse coronary vasoconstriction (Figure 5A and 5B), whereas on day 52, the hyperconstrictions were no longer noted (Figure 5C and 5D). On day 8 and 52, hydroxyfasudil again inhibited the serotonin-induced coronary vasoconstriction and the decrease in coronary blood flow (Figure 5E through 5G).

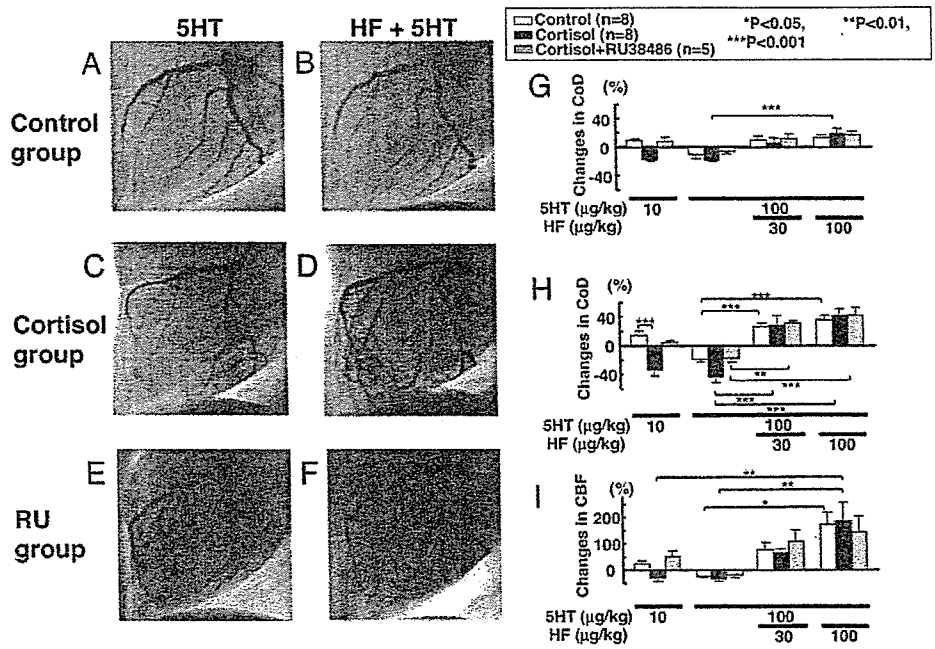

Figure 3. Inhibitory effects of hydroxyfasudil on serotonin-induced coronary vasospasm. Serotonin (5HT) (10 and 100 μg/kg, IC) caused hyperconstriction in both large (G) and small (H) coronary arteries in the cortisol (C) but not in the control (A) or RU (E) group. Hydroxyfasudil (HF) (100 μg/kg, IC) abolished the serotonin-induced vasoconstriction and converted the vasoconstriction to vasodilatation in all groups (B, D, F, G, and H). Similarly, HF converted the serotonin-induced reduction in coronary flow to an increase in the flow in the cortisol group (I). CoD indicates coronary diameter; CBF, coronary blood flow. Results are expressed as mean±SEM.

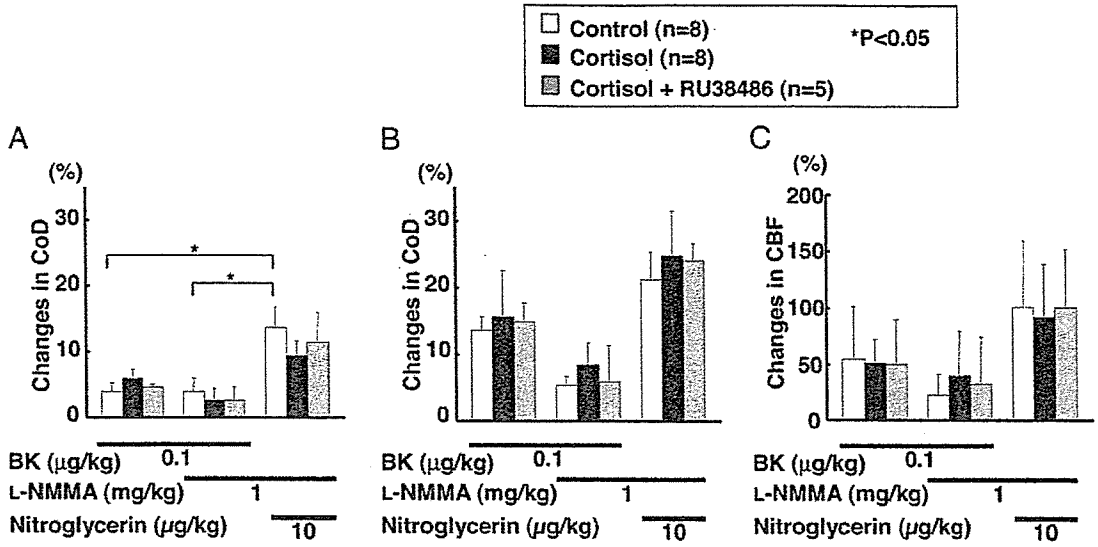

Figure 4. Assessment of coronary endothelial vasodilator functions in vivo. Bradykinin (BK) (0.1 μg/kg, IC) caused a comparable extent of coronary vasodilatation in both large (A) and small (B) coronary arteries and coronary flow (C) among the 3 groups. L-NMMA did not significantly inhibit the bradykinin-induced coronary vasodilatation in all groups. Intracoronary nitroglycerin (10 μg/kg) also caused a comparable extent of coronary vasodilatation among the 3 groups. CoD indicates coronary diameter; CBF, coronary blood flow. Results are expressed as mean±SEM.

Organ Chamber Experiments

Serotonin caused concentration-dependent contractions of coronary rings without endothelium from both-sized arteries (Figure 6). The extent of the contractions was significantly greater in the cortisol group compared with other 3 groups in both-sized coronary arteries (Figure 6A and 6D). Hydroxyfasudil significantly suppressed the serotonin-induced hypercontractions of both-sized arteries (Figure 6B and 6E). No

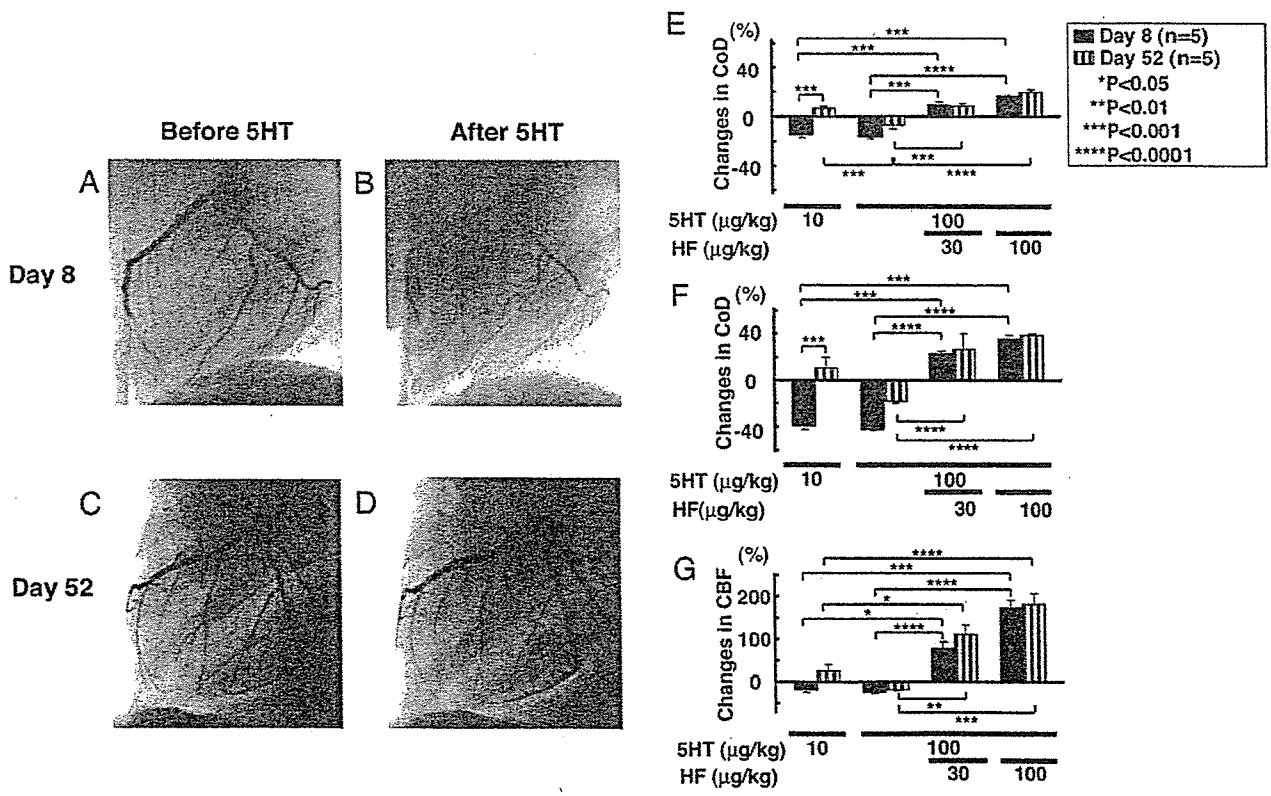

Figure 5. Effects of cessation of chronic cortisol treatment. After confirmation of the serotonin (5HT)-induced coronary vasospasm on day 8 (A and B), the cortisol treatment was stopped. On day 52, the serotonin-induced vasospasm was no longer noted (C and D). Comparisons between day 8 and 52 are shown for coronary vasoconstriction in large (E) and small (F) coronary arteries and coronary flow (G). CoD indicates coronary diameter; CBF, coronary blood flow; HF, hydroxyfasudil. Results are expressed as mean±SEM.

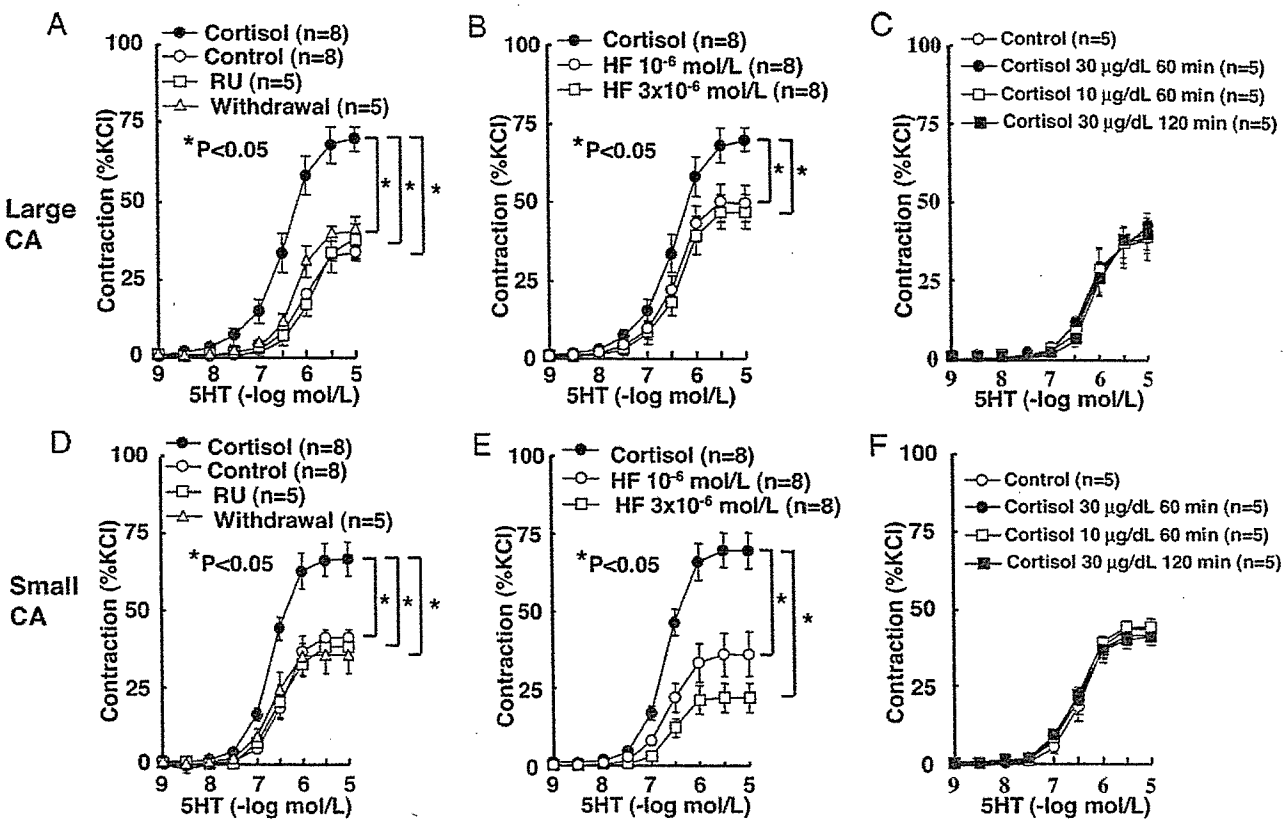

Figure 6. Acute and chronic effects of cortisol on serotonin-induced coronary VSMC contractions in vitro. The chronic cortisol treatment enhanced serotonin-induced VSMC contractions in both large (A) and small (D) coronary arteries (CA) compared with other 3 groups, which were significantly inhibited by hydroxyfasudil (HF) in both large (B) and small (E) coronary arteries. By contrast, no acute effects of the hormone were noted in large (C) or small (F) coronary arteries. Results are expressed as mean±SEM.

acute effects of cortisol on serotonin-induced contractions of normal coronary rings were noted (Figure 6C and 6F).

Endothelium-dependent relaxations to bradykinin were comparable among the 4 groups in both-sized arteries under the 4 different conditions (supplemental Table IV), and no acute effects of cortisol on endothelium-dependent relaxations of normal coronary rings were noted (supplemental Table V). Endothelium-independent relaxations to SNP also were comparable among the 4 groups in both-sized coronary arteries (supplemental Table VI).

Histopathology

There were no obvious histological changes (eg, intimal thickening or inflammatory cell infiltration) in any of the 4 groups (n=5 each, data not shown).

Western Blot Analysis

The extent of MBS phosphorylation, a marker of Rho-kinase activity, was enhanced in response to serotonin only in the cortisol group, and was dose-dependently inhibited by hydroxyfasudil (Figure 7). By contrast, in other 3 groups, the serotonin-induced Rho-kinase activation was absent and no inhibitory effects of hydroxyfasudil were noted (Figure 7). There was a significant positive correlation between the extent of MBS phosphorylation (Rho-kinase activity) and that of the serotonin-induced contractions among the 4 groups studied (Figure 8A) and the inhibitory effects of hydroxyfasudil on the serotonin-induced activation of Rho-kinase was confirmed (Figure 8B).

Discussion

The novel findings of the present study are that sustained elevation of serum cortisol level causes sensitization of coronary VSMC constricting responses to serotonin both in vivo and in vitro and that Rho-kinase–mediated pathway is substantially involved in the molecular mechanisms for the sensitization. To the best of our knowledge, this is the first study that demonstrates the link between elevated serum cortisol level and hyperconstriction of coronary VSMCs through Rho-kinase activation in vivo.

Sustained Elevation of Serum Cortisol Level and Rho-Kinase Activity

We have demonstrated that Rho-kinase is upregulated in spastic coronary segment, which leads to inhibition of myosin light chain (MLC) phosphatase with resultant enhancement of MLC phosphorylation and VSMC contraction.[16,18,26,35] In the present study, we were able to demonstrate that sustained elevation of serum cortisol level enhances coronary vasospastic activity through Rho-kinase activation. Serotonin exerts 5-HT_{2A} serotonergic receptor– and Rho-kinase–mediated direct vasoconstrictor effects and 5-HT_{1B} serotonergic receptor–mediated endothelium-dependent relaxations in porcine coronary arteries.[36] In the present study, a specific Rho-kinase

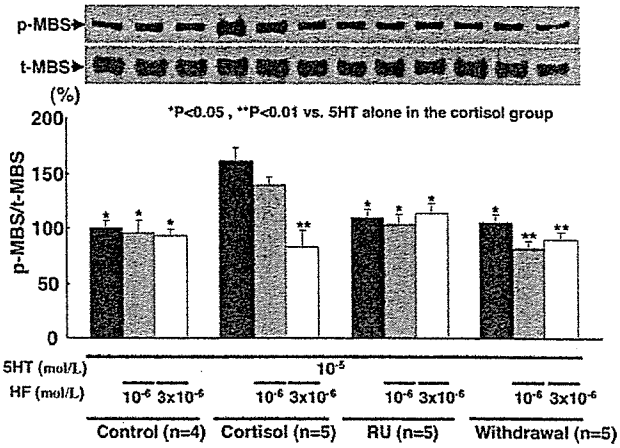

Figure 7. Cortisol-induced Rho-kinase activation in coronary VSMCs. Rho-kinase activity, as evaluated by phosphorylated MBS/total MBS ratio, was significantly enhanced in the cortisol group during serotonin-induced contraction compared with other 3 groups, which was concentration-dependently inhibited by hydroxyfasudil (HF). Results are expressed as mean±SEM.

inhibitor, hydroxyfasudil, unmasked endothelium-dependent vasodilatation and increase in coronary blood flow in response to serotonin through inhibition of the Rho-kinase–mediated direct vasoconstrictor effects of the monoamine.

In this study, the cortisol treatment was stopped 24 hours before the experiment to avoid any acute effects of the hormone. Moreover, cortisol had no acute effect on coronary vasoconstricting responses in vitro. Thus, the sensitization of coronary vasoconstricting responses is apparently attributable to chronic effects of cortisol on Rho-kinase activity in coronary VSMCs.[16,18,26,35] The finding that withdrawal of cortisol resulted in the disappearance of coronary hyperconstricting responses both in vivo and in vitro associated with normalization of coronary Rho-kinase activity further supports this notion.

In the present study, endothelial vasodilator function per se was preserved, whereas VSMC contraction was enhanced in response to the chronic elevation of serum cortisol level in both-sized coronary arteries. However, the decrease in coronary flow secondary to enhanced vasoconstriction in coronary resistance vessels could, at the same time, amplify the net vasoconstriction by reducing shear stress induced vascular relaxation. The mechanism for the enhanced coronary vasoconstricting responses caused by sustained elevation of serum cortisol level is apparently attributable to VSMC hyperreactivity that exceeds endothelial vasodilator capacity, a consistent finding with our previous studies.[25,35,36] In the present study, coronary endothelial vasodilator function in response to bradykinin was relatively resistant to the blockade of NO synthesis in both-sized arteries both in vivo and in vitro. This finding also is consistent with our previous findings that endothelium-dependent relaxation to bradykinin is largely mediated by EDHF.[20,37] However, it remains to be examined whether EDHF-mediated responses also are impaired in response to a long-term increase in serum cortisol levels.

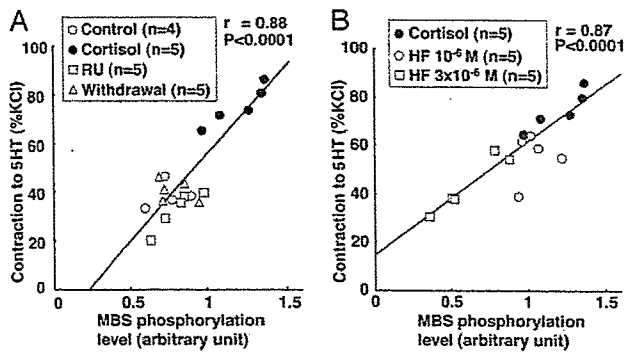

Figure 8. Correlation between the extent of MBS phosphorylation and that of serotonin-induced contractions in the control, cortisol, RU, and withdrawal groups (A) and in the absence (cortisol) and presence of hydroxyfasudil (HF) (B). There were significant positive correlations between the 2 values.

Cortisol and CAD

There is a line of evidence for the link between cortisol and CAD. The 5-year incidence of cardiovascular events was significantly higher in men with abnormal cortisol secretion compared with those with a normal pattern.[38] In addition, increased serum cortisol level in patients with depression enhances prothrombotic state[2] and increases the density of 5-HT_2 serotonergic receptors in platelets, a useful index of platelet activation.[39] Cortisol also could accelerate atherosclerotic process[40]; however, no atherosclerotic changes were noted in the present study, probably because of the relatively short treatment period.

Role of Cortisol in the Pathogenesis of Stress-Induced CAD

Environmental and/or psychological factors contribute to the pathogenesis of CAD.[1–4] It is known that serum levels of cortisol are frequently and chronically elevated in humans with stress and are also normalized after stress is resolved.[41–44] Indeed, natural and/or social disasters have been associated with a transient increase in ischemic cardiac events after the disasters.[45–48]

Coronary vasospasm could be induced in either a focal form or a diffuse form.[36] The latter form may be more frequently associated with myocardial ischemia because of more increased coronary vascular resistance.[36] In the present study, the sustained increase in serum cortisol level sensitized coronary VSMC constricting responses and caused a diffuse form of coronary vasospasm with myocardial ischemia, suggesting an increased risk of myocardial ischemia and sudden death in stress.

Cortisol is secreted by the activated hypothalamic/pituitary/adrenal axis and plays a key role in stress.[11,12] Elevated plasma and urinary levels of corticosteroids and a disturbed diurnal cortisol rhythm have been documented in a variety of diseases with mental stress, including depression, which is among the important risk factors of cardiovascular disease.[10–12] Stress may be closely related to vasospastic angina[6,8]; however, no direct evidence has yet been provided for the link between stress and coronary vasospasm. The present study suggests that Rho-kinase–mediated sensitization of coronary VSMC constricting responses caused by elevated

serum cortisol level is involved in the increased risk of CAD in stressful environments.

Limitations of the Study

Several limitations should be mentioned for the present study. First, we did not directly examine the effects of stress on coronary artery responsiveness. In a preliminary study, we actually attempted to induce a long-lasting stress in pigs; however, continuous restraint in a small cage did not cause sustained elevation of cortisol, indicating that the animals adapted to the restraint stress. In addition, intermittent restraint stress caused elevation of cortisol level; however, this elevation also declined in several days. This point should be examined in a future study. Second, because we only examined the coronary vasomotor responses in pigs, the vascular responsiveness in different organs, different species, and different stage of vascular disease remain to be examined. Third, the detailed molecular mechanisms for the cortisol-induced Rho-kinase activation remain to be examined. Fourth, the effects of cortisol on coronary vascular responses to agonists other than serotonin remain to be examined. However, the use of serotonin was justified as a vasoconstrictor of the coronary arteries in humans.[49] Moreover, because we have previously demonstrated that serotonin and many other vasoconstrictors use Rho-kinase pathway for their vasoconstrictor effects,[19,38] it is possible that coronary vasoconstricting responses to many other agonists also are enhanced when serum cortisol level is chronically elevated.

Clinical Implications

The present study provides the direct evidence for the role of sustained elevation of serum cortisol level in the pathogenesis of coronary vasospasm through activation of Rho-kinase. Importantly, the cessation of the cortisol administration normalized both the coronary vasoconstricting responses and Rho-kinase activity. Thus, the present results suggest that effective management of stress is crucial for the prevention of coronary vasospasm and that a specific Rho-kinase inhibitor may be useful to inhibit the stress-induced ischemic cardiovascular events in humans.

Acknowledgments

We thank M. Sonoda, Y. Matsuo, Y. Murayama, E. Gunshima, and N. Shintani for excellent technical assistance. We also thank Asahi Kasei Pharma Corporation (Tokyo, Japan) for providing hydroxyfasudil.

Sources of Funding

This work was supported in part by the grants-in-aid from the Japanese Ministry of Education, Culture, Sports, Science and Technology (nos. 15256003 and 16209027); the Program for Promotion of Fundamental Studies in Health Sciences of the Organization for Pharmaceutical Safety and Research of Japan; and the Japan Science and Technology Agency, Core Research for Evolutional Science and Technology. H.S. is the recipient of the 2006 Jeffrey M. Hoeg Arteriosclerosis, Thrombosis, and Vascular Biology Award of the American Heart Association.

Disclosures

None.

References

1. Gullette EC, Blumenthal JA, Babyak M, Jiang W, Waugh RA, Frid DJ, O'Connor CM, Morris JJ, Krantz DS. Effects of mental stress on myocardial ischemia during daily life. *JAMA*. 1997;277:1521–1526.
2. Musselman DL, Evans DL, Nemeroff CB. The relationship of depression to cardiovascular disease: epidemiology, biology, and treatment. *Arch Gen Psychiatry*. 1998;55:580–592.
3. Rozanski A, Blumenthal JA, Kaplan J. Impact of psychological factors on the pathogenesis of cardiovascular disease and implications for therapy. *Circulation*. 1999;99:2192–2217.
4. Strike PC, Steptoe A. Psychosocial factors in the development of coronary artery disease. *Prog Cardiovasc Dis*. 2004;46:337–347.
5. Blumenthal JA, Jiang W, Waugh RA, Frid DJ, Morris JJ, Coleman RE, Hanson M, Babyak M, Thyrum ET, Krantz DS, O'Connor C. Mental stress-induced ischemia in the laboratory and ambulatory ischemia during daily life. Association and hemodynamic features. *Circulation*. 1995;92:2102–2108.
6. Numata Y, Ogata Y, Oike Y, Matsumura T, Shimada K. A psychobehavioral factor, alexithymia, is related to coronary spasm. *Jpn Circ J*. 1998;62:409–413.
7. Rozanski A, Bairey CN, Krantz DS, Friedman J, Resser KJ, Morell M, Hilton-Chalfen S, Hestrin L, Bietendorf J, Berman DS. Mental stress and the induction of silent myocardial ischemia in patients with coronary artery disease. *N Engl J Med*. 1988;318:1005–1012.
8. Yoshida K, Utsunomiya T, Morooka T, Yazawa M, Kido K, Ogawa T, Ryu T, Ogata T, Tsuji S, Tokushima T, Matsuo S. Mental stress test is an effective inducer of vasospastic angina pectoris: comparison with cold pressor, hyperventilation and master two-step exercise test. *Int J Cardiol*. 1999;70:155–163.
9. Broadley AJ, Korszun A, Abdelaal E, Moskvina V, Jones CJ, Nash GB, Ray C, Deanfield J, Frenneaux MP. Inhibition of cortisol production with metyrapone prevents mental stress-induced endothelial dysfunction and baroreflex impairment. *J Am Coll Cardiol*. 2005;46:344–350.
10. Butler PW, Besser GM. Pituitary-adrenal function in severe depressive illness. *Lancet*. 1968;291:1234–1236.
11. Lundberg U. Stress hormones in health and illness: the roles of work and gender. *Psychoneuroendocrinology*. 2005;30:1017–1021.
12. McEwen BS. Mood disorders and allostatic load. *Biol Psychiatry*. 2003;54:200–207.
13. Johns DG, Dorrance AM, Tramontini NL, Webb RC. Glucocorticoids inhibit tetrahydrobiopterin-dependent endothelial function. *Exp Biol Med (Maywood)*. 2001;226:27–31.
14. Mangos GJ, Walker BR, Kelly JJ, Lawson JA, Webb DJ, Whitworth JA. Cortisol inhibits cholinergic vasodilation in the human forearm. *Am J Hypertens*. 2000;13:1155–1160.
15. Mitchell BM, Dorrance AM, Webb RC. GTP cyclohydrolase 1 downregulation contributes to glucocorticoid hypertension in rats. *Hypertension*. 2003;41:669–674.
16. Kandabashi T, Shimokawa H, Miyata K, Kunihiro I, Kawano Y, Fukata Y, Higo T, Egashira K, Takahashi S, Kaibuchi K, Takeshita A. Inhibition of myosin phosphatase by upregulated rho-kinase plays a key role for coronary artery spasm in a porcine model with interleukin-1b. *Circulation*. 2000;101:1319–1323.
17. Kandabashi T, Shimokawa H, Mukai Y, Matoba T, Kunihiro I, Morikawa K, Ito M, Takahashi S, Kaibuchi K, Takeshita A. Involvement of Rho-kinase in agonists-induced contractions of arteriosclerotic human arteries. *Arterioscler Thromb Vasc Biol*. 2002;22:243–248.
18. Masumoto A, Mohri M, Shimokawa H, Urakami L, Usui M, Takeshita A. Suppression of coronary artery spasm by the Rho-kinase inhibitor fasudil in patients with vasospastic angina. *Circulation*. 2002;105:1545–1547.
19. Shimokawa H, Ito A, Fukumoto Y, Kadokami T, Nakaike R, Sakata M, Takayanagi T, Egashira K, Takeshita A. Chronic treatment with interleukin-1β induces coronary intimal lesions and vasospastic responses in pigs in vivo. The role of platelet-derived growth factor. *J Clin Invest*. 1996;97:769–776.
20. Shimokawa H, Morikawa K. Hydrogen peroxide is an endothelium-derived hyperpolarizing factor in animals and humans. *J Mol Cell Cardiol*. 2005;39:725–732.
21. Loijens LW, Schouten WG, Wiepkema PR, Wiegant VM. Brain opioid receptor density reflects behavioral and heart rate responses in pigs. *Physiol Behav*. 2002;76:579–587.
22. van der Beek EM, Wiegant VM, Schouten WG, van Eerdenburg FJ, Loijens LW, van der Plas C, Benning MA, de Vries H, de Kloet ER, Lucassen PJ. Neuronal number, volume, and apoptosis of the left dentate

gyrus of chronically stressed pigs correlate negatively with basal saliva cortisol levels. *Hippocampus*. 2004;14:688–700.
23. Kudielka BM, Schommer NC, Hellhammer DH, Kirschbaum C. Acute HPA axis responses, heart rate, and mood changes to psychosocial stress (TSST) in humans at different times of day. *Psychoneuroendocrinology*. 2004;29:983–992.
24. Flynn NE, Wu G. Glucocorticoids play an important role in mediating the enhanced metabolism of arginine and glutamine in enterocytes of post-weaning pigs. *J Nutr*. 1997;127:732–737.
25. Miyata K, Shimokawa H, Yamawaki T, Kunihiro I, Zhou X, Higo T, Tanaka E, Katsumata N, Egashira K, Takeshita A. Endothelial vasodilator function is preserved at the spastic/inflammatory coronary lesions in pigs. *Circulation*. 1999;100:1432–1437.
26. Shimokawa H, Seto M, Katsumata N, Amano M, Kozai T, Yamawaki T, Kuwata K, Kandabashi T, Egashira K, Ikegaki I, Asano T, Kaibuchi K, Takeshita A. Rho-kinase-mediated pathway induces enhanced myosin light chain phosphorylations in a swine model of coronary artery spasm. *Cardiovasc Res*. 1999;43:1029–1039.
27. Kanazawa K, Suematsu M, Ishida T, Hirata K, Kawashima S, Akita H, Yokoyama M. Disparity between serotonin- and acetylcholine-provoked coronary artery spasm. *Clin Cardiol*. 1997;20:146–152.
28. Doucette JW, Corl PD, Payne HM, Flynn AE, Goto M, Nassi M, Segal J. Validation of a Doppler guide wire for intravascular measurement of coronary artery flow velocity. *Circulation*. 1992;85:1899–1911.
29. Shimokawa H, Vanhoutte PM. Dietary cod-liver oil improves endothelium-dependent responses in hypercholesterolemic and atherosclerotic porcine coronary arteries. *Circulation*. 1988;78:1421–1430.
30. Matoba T, Shimokawa H, Nakashima M, Hirakawa Y, Mukai Y, Hirano K, Kanaide H, Takeshita A. Hydrogen peroxide is an endothelium-derived hyperpolarizing factor in mice. *J Clin Invest*. 2000;106:1521–1530.
31. Morikawa K, Shimokawa H, Matoba T, Kubota H, Akaike T, Talukder MA, Hatanaka M, Fujiki T, Maeda H, Takahashi S, Takeshita A. Pivotal role of Cu,Zn-superoxide dismutase in endothelium-dependent hyperpolarization. *J Clin Invest*. 2003;112:1871–1879.
32. Miyata K, Shimokawa H, Kandabashi T, Higo T, Morishige K, Eto Y, Egashira K, Kaibuchi K, Takeshita A. Rho-kinase is involved in macrophage-mediated formation of coronary vascular lesions in pigs in vivo. *Arterioscler Thromb Vasc Biol*. 2000;20:2351–2358.
33. Kaibuchi K, Kuroda S, Amano M. Regulation of the cytoskeleton and cell adhesion by the Rho family GTPases in mammalian cells. *Annu Rev Biochem*. 1999;68:459–486.
34. Kimura K, Ito M, Amano M, Chihara K, Fukata Y, Nakafuku M, Yamamori B, Feng J, Nakano T, Okawa K, Iwamatsu A, Kaibuchi K. Regulation of myosin phosphatase by Rho and Rho-associated kinase (Rho-kinase). *Science*. 1996;273:245–248.
35. Shimokawa H, Takeshita A. Rho-kinase is an important therapeutic target in cardiovascular medicine. *Arterioscler Thromb Vasc Biol*. 2005;25:1767–1775.
36. Shimokawa H. Cellular and molecular mechanisms of coronary artery spasm: lessons from animal models. *Jpn Circ J*. 2000;64:1–12.
37. Matoba T, Shimokawa H, Morikawa K, Kubota H, Kunihiro I, Urakami-Harasawa L, Mukai Y, Hirakawa Y, Akaike T, Takeshita A. Electron spin resonance detection of hydrogen peroxide as an endothelium-derived hyperpolarizing factor in porcine coronary microvessels. *Arterioscler Thromb Vasc Biol*. 2003;23:1224–1230.
38. Rosmond R, Wallerius S, Wanger P, Martin L, Holm G, Bjorntorp P. A 5-year follow-up study of disease incidence in men with an abnormal hormone pattern. *J Intern Med*. 2003;254:386–390.
39. Biegon A, Essar N, Israeli M, Elizur A, Bruch S, Bar-Nathan AA. Serotonin 5-HT2 receptor binding on blood platelets as a state dependent marker in major affective disorder. *Psychopharmacology (Berl)*. 1990;102:73–75.
40. Eller NH, Netterstrom B, Allerup P. Progression in intima media thickness—the significance of hormonal biomarkers of chronic stress. *Psychoneuroendocrinology*. 2005;30:715–723.
41. Rubin RT, Rahe RH, Arthur RJ, Clark BR. Adrenal cortical activity changes during underwater demolition team training. *Psychosom Med*. 1969;31:553–564.
42. Rubin RT, Rahe RH, Clark BR, Arthur RJ. Serum uric acid, cholesterol, and cortisol levels. Interrelationships in normal men under stress. *Arch Intern Med*. 1970;125:815–819.
43. Rahe RH, Rubin RT, Arthur RJ. The three investigators study. Serum uric acid, cholesterol, and cortisol variability during stresses of everyday life. *Psychosom Med*. 1974;36:258–268.
44. Leedy MG, Wilson MS. Testosterone and cortisol levels in crewmen of U.S. Air Force fighter and cargo planes. *Psychosom Med*. 1985;47:333–338.
45. Goldberg RJ, Spencer F, Lessard D, Yarzebski J, Lareau C, Gore JM. Occurrence of acute myocardial infarction in Worcester, Massachusetts, before, during, and after the terrorists attacks in New York City and Washington, DC, on 11 September 2001. *Am J Cardiol*. 2005;95:258–260.
46. Kloner RA, Leor J, Poole WK, Perritt R. Population-based analysis of the effect of the Northridge Earthquake on cardiac death in Los Angeles County, California. *J Am Coll Cardiol*. 1997;30:1174–1180.
47. Meisel SR, Kutz I, Dayan KI, Pauzner H, Chetboun I, Arbel Y, David D. Effect of Iraqi missile war on incidence of acute myocardial infarction and sudden death in Israeli civilians. *Lancet*. 1991;338:660–661.
48. Ogawa K, Tsuji I, Shiono K, Hisamichi S. Increased acute myocardial infarction mortality following the 1995 Great Hanshin-Awaji earthquake in Japan. *Int J Epidemiol*. 2000;29:449–455.
49. Leineweber K, Bose D, Vogelsang M, Haude M, Erbel R, Heusch G. Intense vasoconstriction in response to aspirate from stented saphenous vein aortocoronary bypass grafts. *J Am Coll Cardiol*. 2006;47:981–986.

Angiotensin II Type 1 Receptor Blockade Attenuates In-Stent Restenosis by Inhibiting Inflammation and Progenitor Cells

Kisho Ohtani, Kensuke Egashira, Yoshiko Ihara, Kaku Nakano, Kouta Funakoshi, Gang Zhao, Masataka Sata, Kenji Sunagawa

Abstract—The precise mechanism by which angiotensin II type 1 receptor blocker reduces in-stent restenosis in clinical trials is unclear. We, therefore, investigated the mechanism of in-stent neointima formation. Male cynomolgus monkeys and rabbits were fed a high-cholesterol diet and were allocated to untreated control and type 1 receptor blocker groups. Five days after grouping, multilink stents were implanted in the iliac artery. The type 1 receptor blocker reduced the development of in-stent neointima formation by ≈30% in rabbits and monkeys. To investigate potential mechanisms, we examined the expression of renin–angiotensin system markers, all of which increased in monocytes and smooth muscle-like cells in the neointima and media within 7 days. The type 1 receptor blocker attenuated increased oxidative stress, the enhanced expression of markers of the rennin–angiotensin system and monocyte chemoattractant protein-1, and macrophage infiltration. The effects of type 1 receptor blocker on the differentiation of peripheral blood mononuclear cells into vascular progenitor cells were also examined. Treatment with type 1 receptor blocker suppressed the enhanced differentiation to smooth muscle progenitor cells induced by stenting. The type 1 receptor blocker attenuated in-stent neointima formation by inhibiting redox-sensitive inflammatory changes and by reducing recruitment of the progenitor cells. These potential actions of type 1 receptor blocker on inflammation and progenitor cells constitute a novel mechanism of suppression of in-stent restenosis by type 1 receptor blocker. (***Hypertension.* 2006;48:664-670.)**

Key Words: angiotensin II ■ oxidative stress ■ monocytes

Coronary intervention with metal stent implantation is performed in >1.5 million patients with atherothrombotic lesions worldwide and has become the major revascularization technique.[1] The clinical benefits of this procedure are reduced by in-stent restenosis. In-stent restenosis results exclusively from neointima formation because of proliferation/migration of smooth muscle cells and inflammatory changes in response to stent-associated injury.[2] Recent clinical trials demonstrated great benefits of drug-eluting stents (containing sirolimus, paclitaxel, etc) in preventing restenosis and improving clinical outcomes.[3,4] However, systemic medical therapies for stent-associated thrombosis and for control of risk factors are essential therapy in addition to drug-eluting stents for the prevention of future coronary events. This notion is supported by recent reports showing multiple atherosclerotic plaque ruptures at sites other than the culprit lesion, as observed in acute coronary syndrome by intravascular ultrasound analysis.[5] The renin–angiotensin system (RAS) has been implicated in the pathogenesis of restenosis and acute coronary syndrome[6–11] and, thus, may be a potential target for the prevention of in-stent restenosis and atherothrombotic events. Indeed, a recent, single-center VALsartan for Prevention of REstenosis after Stenting of Type B2/C lesions (Val-PREST) trial demonstrated that treatment with angiotensin II type 1 (AT_1) receptor blocker (ARB) reduces the incidence of restenosis and revascularization in selected patients with type B2/C lesions.[12] The same group compared valsartan with angiotensin-converting enzyme (ACE) inhibition after bare metal stent implantation in the VALsartan Versus ACE inhibition (VALVACE) trial and reported greater benefits from systemic valsartan treatment than from angiotensin-converting enzyme inhibitors in reducing restenosis.[13]

However, the precise mechanism by which ARB reduces in-stent restenosis in Val-PREST and VALVACE trials is unclear. Although the central role of RAS in the pathogenesis of atherosclerotic vascular disease is evident, the role of RAS in the pathogenesis of in-stent neointimal formation has not been fully addressed. For example, upregulation of ACE is reported in postballoon restenotic samples,[14] but no previous study examined the expression of RAS components (ACE, angiotensin II, AT_1 receptor,

Received May 1, 2006; first decision June 2, 2006; revision accepted July 14, 2006.

From the Department of Cardiovascular Medicine (K.O., K.E., G.Z., Y.I., K.F., K.N., K.S.), Graduate School of Medical Sciences, Kyushu University, Fukuoka, Japan; and the Department of Cardiovascular Medicine (M.S.), Graduate School of Medical Sciences, University of Tokyo, Tokyo, Japan.

Correspondence to Kensuke Egashira, Department of Cardiovascular Medicine Graduate School of Medical Science, Kyushu University, 3-1-1, Maidashi, Higashi-ku, Fukuoka 812-8582, Japan. E-mail egashira@cardiol.med.kyushu-u.ac.jp

Hypertension **is available at http://www.hypertensionaha.org** **DOI: 10.1161/01.HYP.0000237974.74488.30**

and AT_2 receptor) and subsequent cellular events after stenting. This point is important because: (1) the mechanism underlying neointimal formation differs considerably between injury methods, and (2) metallic stent implantation now becomes the major revascularization technique. Therefore, the first aim of the present study was to determine the effects of ARB on experimental in-stent restenotic lesions. To gain clinical significance for the results, we used a nonhuman primate model of in-stent neointima formation.[15] We then aimed to investigate the underlying mechanism in a rabbit model. We demonstrate that: (1) increases in local expression of RAS begin at early stages after stenting, and (2) treatment with ARB attenuates in-stent neointima formation associated with reduction in oxidative stress, inflammatory changes, and AT_1 receptor expression.

There is accumulating evidence from experimental studies that vascular smooth muscle cells within the neointima of the atherosclerotic vessel wall may originate from bone marrow.[16] Furthermore, a recent study demonstrated that smooth muscle progenitor cells (SMPCs) are present in circulating human blood[17] and that bone marrow-derived smooth muscle cells are highly represented in the intima of human atherosclerotic vessels.[18] Angiotensin II reportedly enhances the proliferation and differentiation of myeloid precursors from $CD34^+$ hematopoietic stem cells through interaction with the AT_1 receptor on $CD34^+$ cells.[19,20] Thus, it is possible that RAS is involved in recruitment and differentiation of bone marrow cells to SMPCs. Therefore, the second aim of this study was to investigate the effects of ARB on the differentiation of peripheral blood mononuclear leukocytes to SMPCs after stenting in rabbits.

Methods

Animal Model of In-Stent Restenosis

The study protocol was reviewed and approved by the Committee on Ethics on Animal Experiments, Kyushu University Faculty of Medicine, and the experiments were conducted according to the

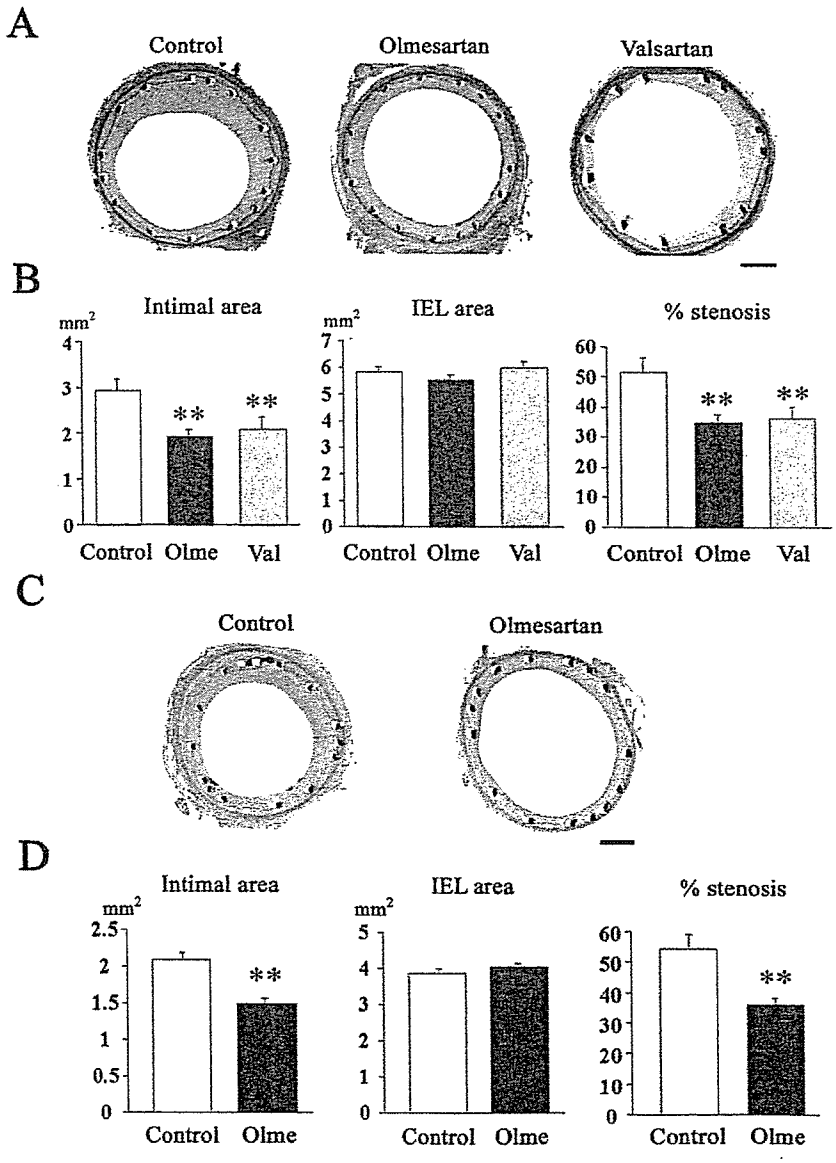

Figure 1. Inhibitory effect of ARB on in-stent neointima formation in monkeys (a and b) and rabbits (c and d). a, Iliac artery sections from the control group, the olmesartan group, and the valsartan group 28 days after stenting, stained with elastic-van-Gieson in monkeys. Bar=500 μm. b, Effect of olmesartan and valsartan on intimal area, IEL area, and % stenosis 28 days after stenting in monkeys (n=8 each). $^{**}P<0.01$ vs the control group. c, Iliac artery sections from the control group and the olmesartan group 28 days after stenting, stained with elastic-van-Gieson in rabbits. Bar=500 μm. d, Effect of olmesartan on intimal area, internal elastic lamina (IEL) area, and % stenosis 28 days after stenting in rabbits (n=8 each). $^{**}P<0.01$ vs the control group.

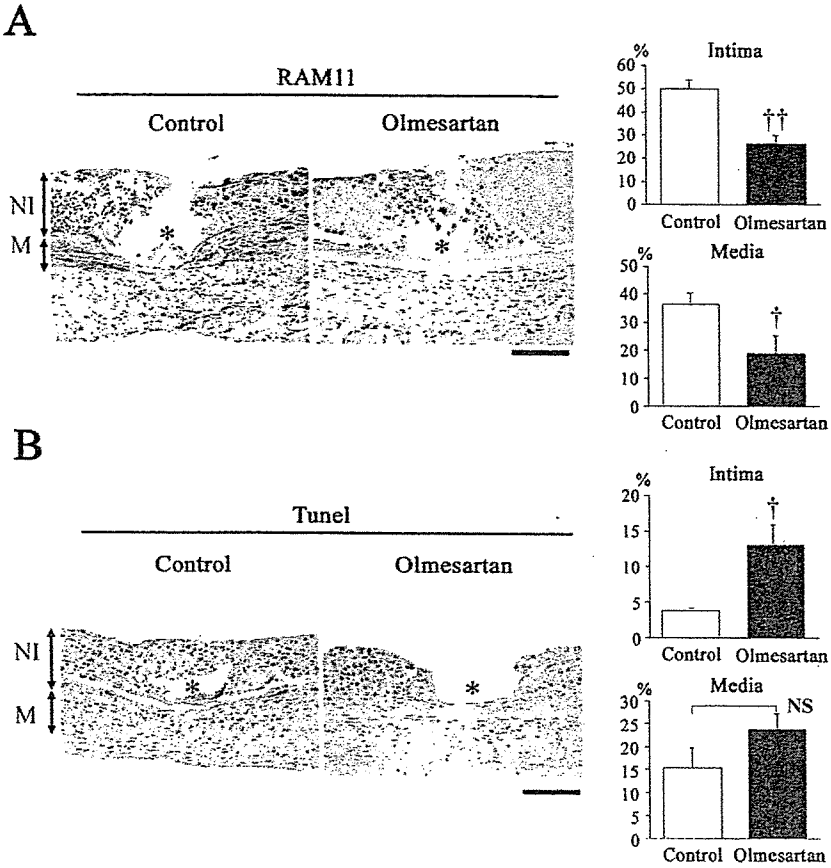

Figure 2. Effects of ARB on inflammation and cell death in rabbits. a, Effect of olmesartan on inflammation (RAM11-positive monocyte/macrophage) 7 days after stenting (n=8 each). Summary of quantitative analyses is presented in bar graph. The percentage of immunopositive cells per total cells in each section was calculated, and the average of the 5 sections was reported for each animal. †$P<0.05$, ††$P<0.01$ vs the control group. * indicates stent strut; NI, neointima; M, media. Bar=100 μm. b, Effects of olmesartan on cell death. TUNEL-stained artery sections 7 days after stenting and summary of quantitative analyses are presented (n=8 each). The percentage of immunopositive cells per total cells in each section was calculated, and the average of the 5 sections was reported for each animals. †$P<0.01$ vs the control group. * indicates stent strut; NI, neointima; M, media. Bar=100 μm.

National Institutes of Health Guide for the Care and Use of Laboratory Animals. An enhanced Methods section is available online at http://hyper.ahajournals.org.

Results

Inhibitory Effects of ARBs on Neointima Formation After Stenting in Monkeys and Rabbits

As we reported previously,[15] significant neointima formation was observed 28 days after stenting in control, untreated monkeys (Figure 1). Treatment with olmesartan or valsartan reduced this neointima formation.

Neointima formation was also examined 28 days after stenting in rabbits (Figure 2). Treatment with olmesartan reduced the degree of neointima formation to a similar extent as seen in monkeys. As expected, serum angiotensin II levels rose on day 28 in the olmesartan group (data not shown).

There were no treatment effects of ARBs on serum cholesterol levels. In monkeys, the total cholesterol levels before and 28 days after stenting were 444±43 and 429±37 mg/dL in the control group, 469±30 and 488±44 mg/dL in the olmesartan-treated group, and 469±30 and 488±44 mg/dL in the valsartan-treated group. In rabbits, the total cholesterol levels before and 28 days after stenting were 919±81 and 1072±93 mg/dL in the control group and 997±97 and 1128±108 mg/dL in the olmesartan-treated group. There was no significant treatment effect on body weight among the groups (data not shown).

Inhibitory Effects of ARB on Markers of RAS (ACE, Angiotensin II, AT_1 Receptor, and AT_2 Receptor) and Oxidative Stress After Stent Implantation in Rabbits

To investigate potential mechanisms underlying the beneficial effects of ARBs on in-stent neointima formation, we examined whether markers of RAS are increased after stent implantation in rabbits (Figure I, available online). Immunohistochemical staining revealed that such markers (ACE, angiotensin II, AT_1 receptor, and AT_2 receptor) increased on day 10 in nearly all of the cells in the neointima (regenerated endothelial cells, monocytes, and smooth muscle-like cells) and in some cells in the media (Figure Ia). Such increased immunoreactivity declined spontaneously. Interestingly, treatment with olmesartan reduced the enhanced expression of AT_1 receptor but did not affect the expression of AT_2 receptor (online Figure I).

Because oxidative stress plays a central role in vascular pathobiology induced by angiotensin II, we then examined superoxide production by dihydroethidium (DHE) fluorescence on day 10 (Figure Ic). No apparent DHE fluorescence was detected in the nonstented normal artery. The fluorescent signal was markedly increased in the neointima, media, and adventitia of stented arteries from the control group. Treat-

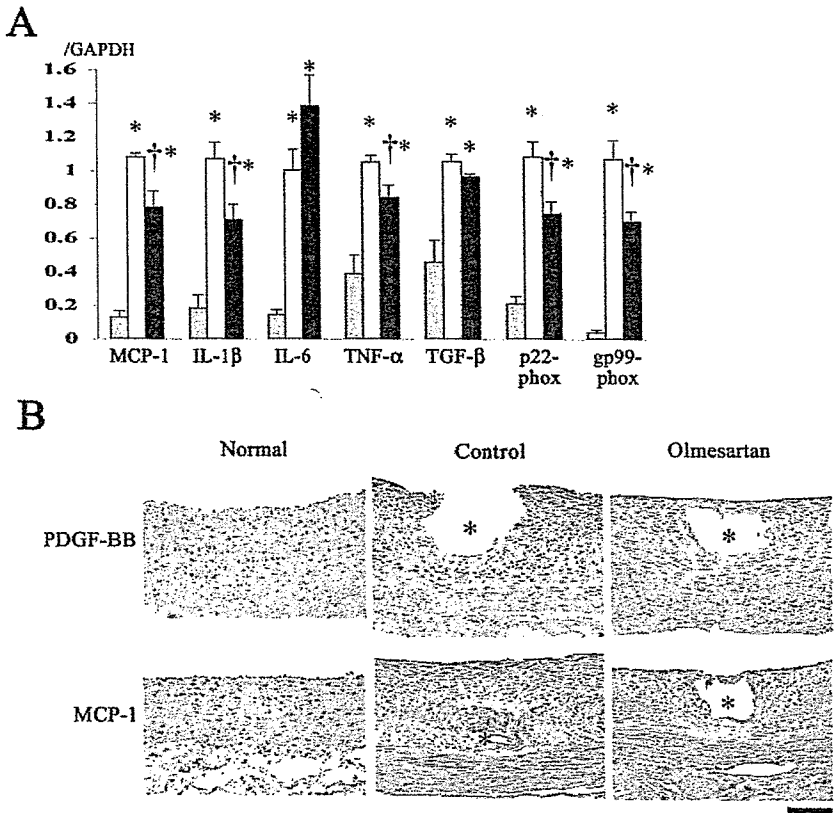

Figure 3. Effects of ARB on gene expression of proinflammatory factors, and immunohistochemical expression of PDGF and MCP-1. a, Effect of olmesartan on relative mRNA levels of various proinflammatory factors and NADPH oxidases 7 days after stenting in normal controls (▨, n=8), the no-treatment group (□, n=8), and the ARB-treated group (■, n=8). *$P<0.01$ vs uninjured normal artery; †$P<0.05$, vs the control group. b, Iliac artery sections from the uninjured normal animals and those from the control and olmesartan groups 10 days after stenting stained immunohistochemically with PDGF-BB and MCP-1. * indicates stent strut. Bar=100 μm. These immunohistochemical experiments were repeated 5 times, all with representative results.

ment with olmesartan partly attenuated the increased DHE fluorescence after stent implantation.

Inhibitory Effects of ARB on Inflammatory Changes and Apoptotic Cell Death in Rabbits

As we reported previously,[15] inflammatory changes and apoptotic cell death became evident 7 to 10 days after stent implantation in rabbits (Figure 2a and 2b). Treatment with olmesartan reduced such inflammatory changes and enhanced cell death in the intima after stenting.

Inhibitory Effects of ARB on Expression of Proinflammatory Factors and NADPH Oxidase Subunits

Treatment with olmesartan reduced the increased mRNA levels of monocyte chemoattractant protein (MCP)-1, interleukin (IL)-1β, tumor necrosis factor-α, p22phox, and gp91phox in rabbits (Figure 3a). Olmesartan did not affect the increased levels of IL-6 and transforming growth factor-β. Immunohistochemical staining performed 10 days after stenting revealed increased immunoreactive platelet-derived growth factor (PDGF)-β and MCP-1 in cells in the neointima and in smooth muscle cells in the media. This was attenuated by olmesartan treatment (Figure 3b). Treatment with olmesartan did not affect neovascularization in the neointima and adventitia or re-endothelialization 28 days after stenting (data not shown).

Effects of ARB on Transdifferentiation of Mononuclear Cells to Vascular Progenitor Cells

To investigate the potential contribution of vascular progenitor cells, peripheral blood mononuclear cells (MNCs) were isolated and cultured to stimulate the differentiation into SMPCs or endothelial progenitor cells (EPCs), as described previously.[16,17] The cells cultured in the PDGF-BB–enriched and basic fibroblast growth factor–enriched medium exhibited a hill and valley morphology that is characteristic of smooth muscle cells within 2 weeks. The smooth muscle cell phenotype was confirmed by immunostaining with antibodies specific for smooth muscle cell markers: SMPCs expressed α-smooth muscle actin (SMA), myosin, and calponin, which were all detected in human coronary artery smooth muscle cells and were not detected in MNCs and Cos-7 cells (data not shown). Expression of α-SMA gene in SMPCs was also confirmed by PCR analysis (data not shown). As reported,[16,17] the expression of inflammatory markers (MCP-1, IL-1β, etc) was greater in SMPCs than in cultured rabbit aortic smooth muscle cells (data not shown). The cells cultured in the vascular endothelial growth factor–enriched medium exhibited the typical cobblestone morphology of EPCs. The EPCs stained positively for von Willebrand factor and VE-cadherin and incorporated acetylated low-density lipoprotein (data not shown).

Analysis of colony-forming areas showed that the degree of transformation to SMPC was greater in MNCs from animals fed a high-cholesterol diet than in those from untreated, normal animals (Figure 4A). The transformation to SMPCs further enhanced in MNCs from animals that underwent stenting. Treatment of rabbits with olmesartan for 5 to 7 days suppressed the increased transformation to SMPCs induced by stenting. In contrast, there were no differences in the degree of transformation to EPCs among the groups. Immunohisto-

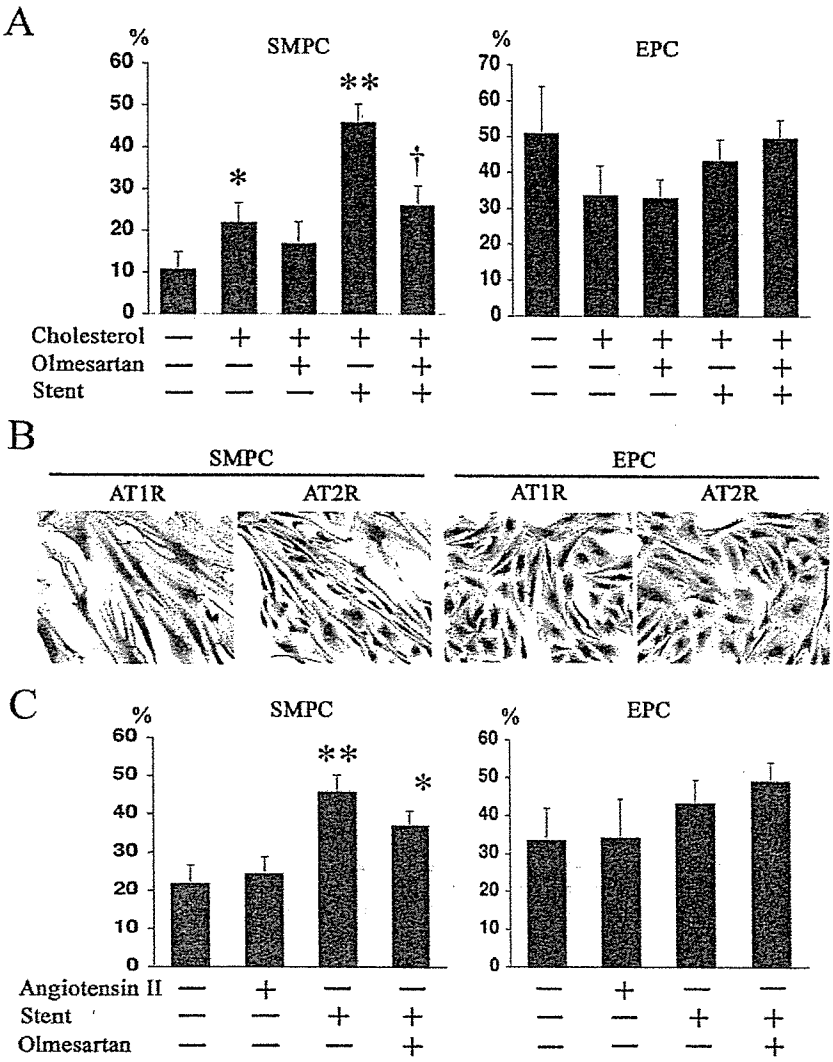

Figure 4. Effects of ARB on transdifferentiation of MNCs to SMPCs or EPCs. a, The degrees of transformation of MNCs to SMPCs (the percentages of α-SMA–positive area per well) or EPCs (the percentages of von Willebrand factor–positive area per well) in normal rabbits and those that received the high-cholesterol diet, high-cholesterol diet plus in vivo olmesartan treatment, high-cholesterol diet and stenting, or high-cholesterol diet, in vivo olmesartan treatment, and stenting (n=8 to 9 each). *P<0.05, **P<0.01 vs control (cholesterol [−] olmesartan [−] stent [−]). †P<0.05 vs high-cholesterol diet plus stenting (cholesterol [+] olmesartan [−] stent [+]). b, Immunohistochemistry for AT1 receptor and AT2 receptor in SMPCs and EPCs. c, The degree of transformation of MNCs from rabbits fed a high-cholesterol diet to SMPCs or EPCs. The effects of in vitro addition of angiotensin II were examined. In addition, the in vitro effects of olmesartan on the stent-induced increase in transformation were examined (n=8 to 9 each). *P<0.05, **P<0.01 vs control (angiotensin II [−] olmesartan [−] stent [−]).

chemical staining was then performed to examine the presence of AT_1 receptor and AT_2 receptor. Both receptors were found in SMPCs and EPCs (Figure 4B). We considered the possibility that AT_1 signals might be involved in increasing the transformation capacity of MNCs and, therefore, examined the effects of in vitro administration of angiotensin II or olmesartan on the transformation of MNCs. Angiotensin II did not enhance transdifferentiation, and olmesartan did not suppress transdiffrentiation in vitro (Figure 4C).

Plasma ARB levels and Arterial Blood Pressure

The maximum drug concentration (C_{max}) levels of olmesartan at 15 mg/kg per day and valsartan at 50 mg/kg per day were 107±17 and 300±24 ng/mL, respectively. The C_{max} level of olmesartan at 3 mg/kg per day was 537±24 ng/mL in rabbits. Therefore, the dose of olmesartan used in rabbits is within a clinically relevant dose range. The C_{max} levels after oral administration of olmesartan at 5, 10, and 20 mg/body in hypertensive subjects are reported to be 149±21, 273±17, and 470±23 ng/mL (n=6, each), respectively. The C_{max} values after oral administration of valsartan at 80 and 160 mg/body in hypertensive subjects are reported to be 2830±920 and 5260±2300 ng/mL, respectively, according to the manufacturer's interview form. Thus, the doses of olmesartan and valsartan used in the present study are within or below the clinically relevant dose range.

Treatment with olmesartan showed no effect on systolic and diastolic arterial pressure. Systolic and diastolic pressure were 94±2 and 59±5 mm Hg in the control group and 92±2 and 52±6 mm Hg in the olmesartan group.

Discussion

We have demonstrated for the first time that oral treatment with 2 types of ARBs (valsartan and olmesartan) attenuated in-stent neointimal formation in nonhuman primates (cynomolgus monkeys), supporting the conclusions of the Val-PREST and VALVACE trials,[12,13] which involved a relatively small number of patients. Although it is uncertain which animal model is most appropriate for the evaluation of in-stent neointima formation (restenotic changes), a nonhuman primate model may have an advantage over nonprimate animal models, because vascular inflammatory and proliferative responses to injury in nonhuman primates are more similar to those in humans than are other, nonprimate models.

Hence, the use of nonhuman primates may work for evaluation of the efficacy of ARB on in-stent neointima formation in clinically relevant conditions.

To obtain mechanistic insight into the beneficial effects of ARB, we first examined the time course of local expression of RAS components in rabbits (Figure 2). We found that expression of all of the components (ACE, angiotensin II, AT_1 receptor, and AT_2 receptor) increased, mainly in cells composed of neointima (monocytes and smooth muscle cells), at early stages (7 to 10 days after stenting), and persisted until 28 days after stenting. This RAS activation colocalized with increased NADPH oxidase–dependent DHE fluorescence (generation of superoxide anion) and was associated with increased levels of NADPH oxidase subunit mRNAs, consistent with previous reports showing that increased reactive oxygen species can be detected in activated smooth muscle cells after balloon injury.[21,22] These in vivo observations are also consistent with previously published in vitro data suggesting that proliferation and migration of smooth muscle cells are critically mediated by oxidative stress via AT_1-mediated activation of NADPH oxidases.[23–29] Interestingly, treatment with ARB not only attenuated the levels of oxidative stress markers but also reduced the level of immunoreactive AT_1. These data suggest the presence of a positive feedback loop in which activation of AT_1 further enhances expression and activity of the AT_1 receptor in vivo, as seen in the present study.

It is known that oxidative stress–induced inflammatory and proliferative processes are central to neointima formation after vascular injury.[24,25] We and others have demonstrated that[1] increased monocyte-mediated inflammation or MCP-1 expression is associated with greater neointima formation after stenting,[26,27] and[2] anti–MCP-1 gene therapy[15,28–30] or administration of blocking antibody against the MCP-1 receptor[31] markedly reduces neointima formation after vascular injury. However, no previous study examined whether or not those inflammatory and proliferative changes after stenting depends on the AT_1 receptor. In the present study, we, therefore, examined the effects of ARB on monocyte recruitment and MCP-1 expression after stenting and found that ARB reduced monocyte/macrophage recruitment, as well as MCP-1 immunoreactivity and gene expression. Furthermore, ARB inhibition increased the expression of growth-promoting factors, such as PDGF and IL-1β. These data suggest that the beneficial effects of ARB may be attributed to the inhibition of oxidative stress–induced inflammatory and proliferative changes.

Recent studies have shown that peripheral blood contains bone marrow-derived progenitor cells, which contribute to neointima formation after injury.[16,18,32] However, the role of RAS in the recruitment/differentiation of progenitor cells into the neointimal cells after stenting has not been addressed. Here we found that differentiation to SMPCs increased in MNCs from rabbits fed a high-cholesterol diet and was further enhanced in those rabbits that had also undergone stenting. Differentiation into EPCs was not affected by either the diet or stenting. In vivo treatment with ARB suppressed the increased differentiation into SMPCs induced by diet or stenting. In contrast, in vitro treatment with angiotensin II or ARB did not affect the capacity to differentiate into SMPCs or EPCs. Therefore, the capacity to recruit or form SMPCs from MNCs after stenting might be determined by an AT1 receptor–mediated pathway in vivo and, thus, contribute to in-stent neointima formation.

It must be mentioned that ARB did not significantly reduced arterial blood pressure in rabbits. Although arterial pressure was not measured in monkeys, the dose of ARB used in the present study is reported to show no effects on arterial blood pressure in monkeys.[33] Plasma ARB level was within or below the clinical range. Furthermore, ARB did not affect serum lipid levels. Therefore, the beneficial effect of ARB on in-stent neointimal formation is likely to be independent of its effects on arterial blood pressure or serum lipid.

Perspectives

This study provides experimental evidence suggesting that oral treatment with ARB at a clinical dose range attenuates in-stent neointima formation in rabbits and nonhuman primates. The beneficial effects were associated with reduced local oxidative stress, reduced expression of MCP-1 and other inflammation-promoting factors, and reduced recruitment/differentiation of SMPCs, suggesting that ARB is of potential clinical benefit in patients who have undergone vascular interventions.

Sources of Funding

This study was supported by Grants-in-Aid for Scientific Research (14657172 and 14207036) from the Ministry of Education, Science, and Culture, Tokyo, Japan; by Health Science Research Grants (Comprehensive Research on Aging and Health, and Research on Translational Research) from the Ministry of Health Labor and Welfare, Tokyo, Japan; and by the Program for Promotion of Fundamental Studies in Health Sciences of the Organization for Pharmaceutical Safety and Research, Tokyo, Japan.

Disclosures

None.

References

1. Topol EJ, Serruys PW. Frontiers in interventional cardiology. *Circulation.* 1998;98:1802–1820.
2. Hoffmann R, Mintz GS, Dussaillant GR, Popma JJ, Pichard AD, Satler LF, Kent KM, Griffin J, Leon MB. Patterns and mechanisms of in-stent restenosis. A serial intravascular ultrasound study. *Circulation.* 1996;94:1247–1254.
3. Holmes DR Jr, Leon MB, Moses JW, Popma JJ, Cutlip D, Fitzgerald PJ, Brown C, Fischell T, Wong SC, Midei M, Snead D, Kuntz RE. Analysis of 1-year clinical outcomes in the SIRIUS trial: a randomized trial of a sirolimus-eluting stent versus a standard stent in patients at high risk for coronary restenosis. *Circulation.* 2004;109:634–640.
4. Stone GW, Ellis SG, Cox DA, Hermiller J, O'Shaughnessy C, Mann JT, Turco M, Caputo R, Bergin P, Greenberg J, Popma JJ, Russell ME. One-year clinical results with the slow-release, polymer-based, paclitaxel-eluting TAXUS stent: the TAXUS-IV trial. *Circulation.* 2004;109:1942–1947.
5. Rioufol G, Finet G, Ginon I, Andre-Fouet X, Rossi R, Vialle E, Desjoyaux E, Convert G, Huret JF, Tabib A. Multiple atherosclerotic plaque rupture in acute coronary syndrome: a three-vessel intravascular ultrasound study. *Circulation.* 2002;106:804–808.
6. Daemen MJ, Lombardi DM, Bosman FT, Schwartz SM. Angiotensin II induces smooth muscle cell proliferation in the normal and injured rat arterial wall. *Circ Res.* 1991;68:450–456.
7. Bell L, Madri JA. Influence of the angiotensin system on endothelial and smooth muscle cell migration. *Am J Pathol.* 1990;137:7–12.
8. Tharaux PL, Chatziantoniou C, Fakhouri F, Dussaule JC. Angiotensin II activates collagen I gene through a mechanism involving the MAP/ER kinase pathway. *Hypertension.* 2000;36:330–336.

9. Ruiz-Ortega M, Lorenzo O, Suzuki Y, Ruperez M, Egido J. Proinflammatory actions of angiotensins. *Curr Opin Nephrol Hypertens.* 2001;10:321–329.
10. Prasad A, Koh KK, Schenke WH, Mincemoyer R, Csako G, Fleischer TA, Brown M, Selvaggi TA, Quyyumi AA. Role of angiotensin II type 1 receptor in the regulation of cellular adhesion molecules in atherosclerosis. *Am Heart J.* 2001;142:248–253.
11. Wolf G. Free radical production and angiotensin. *Curr Hypertens Rep.* 2000;2:167–173.
12. Peters S, Gotting B, Trummel M, Rust H, Brattstrom A. Valsartan for prevention of restenosis after stenting of type B2/C lesions: the VAL-PREST trial. *J Invasive Cardiol.* 2001;13:93–97.
13. Peters S, Trummel M, Meyners W, Koehler B, Westermann K. Valsartan versus ACE inhibition after bare metal stent implantation–results of the VALVACE trial. *Int J Cardiol.* 2005;98:331–335.
14. Ohishi M, Ueda M, Rakugi H, Okamura A, Naruko T, Becker AE, Hiwada K, Kamitani A, Kamide K, Higaki J, Ogihara T. Upregulation of angiotensin-converting enzyme during the healing process after injury at the site of percutaneous transluminal coronary angioplasty in humans. *Circulation.* 1997;96:3328–3337.
15. Ohtani K, Usui M, Nakano K, Kohjimoto Y, Kitajima S, Hirouchi Y, Li XH, Kitamoto S, Takeshita A, Egashira K. Antimonocyte chemoattractant protein-1 gene therapy reduces experimental in-stent restenosis in hypercholesterolemic rabbits and monkeys. *Gene Ther.* 2004;11:1273–1282.
16. Sata M, Saiura A, Kunisato A, Tojo A, Okada S, Tokuhisa T, Hirai H, Makuuchi M, Hirata Y, Nagai R. Hematopoietic stem cells differentiate into vascular cells that participate in the pathogenesis of atherosclerosis. *Nat Med.* 2002;8:403–409.
17. Simper D, Stalboerger PG, Panetta CJ, Wang S, Caplice NM. Smooth muscle progenitor cells in human blood. *Circulation.* 2002;106:1199–1204.
18. Caplice NM, Bunch TJ, Stalboerger PG, Wang S, Simper D, Miller DV, Russell SJ, Litzow MR, Edwards WD. Smooth muscle cells in human coronary atherosclerosis can originate from cells administered at marrow transplantation. *Proc Natl Acad Sci U S A.* 2003;100:4754–4759.
19. Mrug M, Stopka T, Julian BA, Prchal JF, Prchal JT. Angiotensin II stimulates proliferation of normal early erythroid progenitors. *J Clin Invest.* 1997;100:2310–2314.
20. Rodgers KE, Xiong S, Steer R, diZerega GS. Effect of angiotensin II on hematopoietic progenitor cell proliferation. *Stem Cells.* 2000;18:287–294.
21. Nunes GL, Robinson K, Kalynych A, King SB, 3rd, Sgoutas DS, Berk BC. Vitamins C and E inhibit O2- production in the pig coronary artery. *Circulation.* 1997;96:3593–3601.
22. Shi Y, Niculescu R, Wang D, Patel S, Davenpeck KL, Zalewski A. Increased NAD(P)H oxidase and reactive oxygen species in coronary arteries after balloon injury. *Arterioscler Thromb Vasc Biol.* 2001;21:739–745.
23. Lassegue B, Sorescu D, Szocs K, Yin Q, Akers M, Zhang Y, Grant SL, Lambeth JD, Griendling KK. Novel gp91(phox) homologues in vascular smooth muscle cells: nox1 mediates angiotensin II-induced superoxide formation and redox-sensitive signaling pathways. *Circ Res.* 2001;88:888–894.
24. Egashira K. Clinical importance of endothelial function in arteriosclerosis and ischemic heart disease. *Circ J.* 2002;66:529–533.
25. Griendling KK, FitzGerald GA. Oxidative stress and cardiovascular injury: Part II: animal and human studies. *Circulation.* 2003;108:2034–2040.
26. Farb A, Weber DK, Kolodgie FD, Burke AP, Virmani R. Morphological predictors of restenosis after coronary stenting in humans. *Circulation.* 2002;105:2974–2980.
27. Welt FG, Rogers C. Inflammation and restenosis in the stent era. *Arterioscler Thromb Vasc Biol.* 2002;22:1769–1776.
28. Usui M, Egashira K, Ohtani K, Kataoka C, Ishibashi M, Hiasa K, Katoh M, Zhao Q, Kitamoto S, Takeshita A. Anti-monocyte chemoattractant protein-1 gene therapy inhibits restenotic changes (neointimal hyperplasia) after balloon injury in rats and monkeys. *Faseb J.* 2002;16:1838–1840.
29. Egashira K, Zhao Q, Kataoka C, Ohtani K, Usui M, Charo IF, Nishida K, Inoue S, Katoh M, Ichiki T, Takeshita A. Importance of monocyte chemoattractant protein-1 pathway in neointimal hyperplasia after periarterial injury in mice and monkeys. *Circ Res.* 2002;90:1167–1172.
30. Egashira K. Molecular mechanisms mediating inflammation in vascular disease: special reference to monocyte chemoattractant protein-1. *Hypertension.* 2003;41:834–841.
31. Horvath C, Welt FG, Nedelman M, Rao P, Rogers C. Targeting CCR2 or CD18 inhibits experimental in-stent restenosis in primates: inhibitory potential depends on type of injury and leukocytes targeted. *Circ Res.* 2002;90:488–494.
32. Skowasch D, Jabs A, Andrie R, Dinkelbach S, Luderitz B, Bauriedel G. Presence of bone-marrow- and neural-crest-derived cells in intimal hyperplasia at the time of clinical in-stent restenosis. *Cardiovasc Res.* 2003;60:684–691.
33. Takai S, Kim S, Sakonjo H, Miyazaki M. Mechanisms of angiotensin II type 1 receptor blocker for anti-atherosclerotic effect in monkeys fed a high-cholesterol diet. *J Hypertens.* 2003;21:361–369.